T.C.
DOKUZ EYLUL UNIVERSITY
IZMIR INTERNATIONAL
BİYOMEDICINE AND GENOME
INSTITUTE

IDENTIFICATION OF TRANSCRIPTIONAL REGULATORY NETWORKS CHARACTERIZING INVASIVE AND NON-INVASIVE BLADDER CANCER CELL LINES

PERİHAN YAĞMUR

GÜNERİ SÖZERİ

MOLECULAR BIOLOGY AND GENETICS

MASTER OF SCIENCE THESIS

İZMİR-2021

TEZ KODU: DEU.IBG.MSc/2018850002

T.C.
DOKUZ EYLÜL ÜNİVERSİTESİ İZMİR
ULUSLARARASI BİYOTIP VE GENOM
ENSTİTÜSÜ

KASA İNVAZİF OLAN VE OLMAYAN MESANE KANSERİ HÜCRE HATLARINI KARAKTERİZE EDEN TRANSKRİPSYONEL REGÜLASYON AĞLARININ BELİRLENMESİ

MOLEKÜLER BİYOLOJİ VE GENETİK

YÜKSEK LİSANS TEZİ

PERİHAN YAĞMUR GÜNERİ SÖZERİ

Danışman Öğretim Üyesi: Doç. Dr. Şerif ŞENTÜRK
Eş-Danışman: Dr. Serap ERKEK ÖZHAN

TÜBİTAK, 118Z166

(Bu araştırma TÜBİTAK tarafından 118Z166 nolu proje desteği ile desteklenmiştir.)

TEZ KODU: DEU.IBG.MSc/2018850002

Dokuz Eylül Üniversitesi İzmir Uluslararası Biyotıp ve Genom Enstitüsü
Genom Bilimleri ve Moleküler Biyoteknoloji Anabilim Dalı,
Moleküler Biyoloji ve Genetik Yüksek Lisans programı öğrencisi Perihan Yağmur Güneri Sözeri '**KASA İNVAZİF OLAN VE OLMAYAN MESANE KANSERİ HÜCRE HATLARINI KARAKTERİZE EDEN TRANSKRİPSYONEL REGÜLASYON AĞLARININ BELİRLENMESİ'** konulu Yüksek Lisans tezini 25/08/2021 tarihinde başarılı olarak tamamlamıştır.

JURİ BAŞKANI
Doç Dr. Şerif ŞENTÜRK
Dokuz Eylül Üniversitesi
Genom Bilimleri ve Moleküler Biyoteknoloji
Anabilim Dalı

JURİ ÜYESİ
Dr. Ayşe Banu DEMİR
İzmir Ekonomi Üniversitesi
Temel Tıp Bilimleri
Anabilim Dalı

JURİ ÜYESİ
Doç. Dr. Gökhan KARAKÜLAH
Dokuz Eylül Üniversitesi
Genom Bilimleri ve Moleküler Biyoteknoloji
Anabilim Dalı

YEDEK JURİ ÜYESİ
Yar. Doç. Dr. Yavuz OKTAY
Dokuz Eylül Üniversitesi
Genom Bilimleri ve Moleküler
Biyoteknoloji Anabilim Dalı

YEDEK JURİ ÜYESİ
Yar. Doç. Dr. Cihangir YANDIM
İzmir Ekonomi Üniversitesi
Genetik ve Biyomühendislik
Anabilim Dalı

TABLE OF CONTENTS

TABLE INDEX

FIGURE INDEX

ABBREVIATIONS

MIBC…….Muscle Invasive Bladder Cancer

NMIBC…….Non-muscle Invasive Bladder Cancer

ChIP-Seq……Chromatin Immunopreccipitation Followed by Sequencing

ChIP-SICAP……...Selective Isolation of Chromatin Associated Proteins

RIME……..Rapid Immunoprecipitation Mass Spectrometry of Endogenous Proteins

ChIP-MS…….Chromatin Immunoprecipitation Mass Spectrometry

GO……...Gene Ontology

RPKM……..Reads per Kilobase of Transcript

CCLE……...Cancer Cell Lınes Encyclopedia

DepMap……..Cancer Dependency Map

HDAC……..Histone Deacetylase

TURBT……Trans Urethral Resection of the Bladder

CO_2……..Carbon dioxide

dH_2O……Distilled water

FBS……..Fetal Bovine Serum

DOC…….Deoxycholate

NaCl…….Sodium chloride

EDTA……...Ethylenediaminetetraacetic acid

EGTA……...ethylene glycol-bis(β-aminoethyl ether)-N,N,N′,N′-tetraacetic acid

TE…….Tris EDTA

TAE……..Tris acetate EDTA

PBS……..Phosphate buffered saline

$NaHCO_3$……...Sodium bicarbonate

H3K27ac……..Acetylated 27^{th} Lysine of Histone 3

H3K27me3……..Trimethylated 27^{th} Lysine of Histone 3

ATP……...Adenosine Triphosphate

bp……..Base pair

fc……Final concentration

RT…….Room temperature

^{o}C……..Degrees of Celcius

L……Liter

M……...Molarity

mM……Milimolar

g……Gram

µg……..Microgram

ng……..Nanogram

mL……Mililiter

µL……..Microliter

µM……Micromolar

nm……Nanomolar

rpm……Revolutions per minute

ACKNOWLEDGEMENT

I am extremely grateful to my advisors Şerif Şentürk and Serap Erkek Özhan for their assistance at every stage of the thesis. I have done this thesis thanks to Serap Erkek Özhan who let me do this Project, teach me so many things and trained me during my Master's Thesis.

I would like to extend my sincere thanks to my talented friends and co-workers Gülden Özden Yılmaz, Aleyna Eray, Aslı Korkmaz and Burcu Akman for all the help and the valuable friendship.

I cannot begin to express my thanks to my lovely mother, father and sister for all the effort, support and love that they gave during all of my life. I would also like to extend my deepest gratitude to my lovely husband who encourages me all the time and waited for me during my Master's and his unwavering support and belief in me.

IDENTIFICATION OF TRANSCRIPTIONAL REGULATORY NETWORKS CHARACTERIZING INVASIVE AND NON-INVASIVE BLADDER CANCER CELL LINES

Perihan Yağmur Güneri Sözeri, İzmir Uluslararası Biyotıp ve Genom Enstitüsü

ABSTRACT

Bladder cancer is divided into muscle invasive and non-muscle invasive bladder cancer (MIBC and NMIBC) histopathologically however their prognosis and treatment options are different. In this thesis, the transcriptional regulatory mechanisms characterizing MIBC and NMIBC are aimed to be identified.

H3K27ac chromatin immunoprecipitation followed by sequencing (ChIP-Seq) was used to identify group specific enhancers specific to MIBC (5637, HT1376, J82, T24) and NMIBC (RT112, RT4) cell lines. Transcription factor motifs on differential active regulatory regions are identified and possible gene targets were found. Selective Isolation of Chromatin Associated Proteins (ChIP-SICAP) method was used to find co-partner proteins of the transcription factors. FLI1 and FRA1 ChIP-Seq experiments are also done and the target genes were filtered accordingly. Finally, knockdown of the transcription factors characterizing MIBC group was performed.

FLI1 and FRA1 transcription factors are determined to be enriched at MIBC specific enhancers and GRHL2, Tp63 and PPARg transcription factors are found at NMIBC specific enhancers. Predicted target genes of MIBC group were mostly involved “epithelial cell migration” however NMIBC group’s target genes are mainly consisting transcription factors. Integrative analysis of FLI1 and FRA1 ChIP-SICAP and ChIP-Seq and FLI1 and FRA1 knockdown experiments showed that MAP4K4 and FLOT1 genes are the two key target genes regulated by these transcription factors.

Collectively our results uncovered the regulatory landscapes characterizing MIBC and NMIBC. FLI1 and FRA1 are determined as the two prominent transcription factors regulating the genes involved in gain of invasive characteristics.

Key Words: Bladder cancer, epigenetics, gene regulation, invasion

KASA İNVAZİF OLAN VE OLMAYAN MESANE KANSERİ HÜCRE HATLARINI KARAKTERİZE EDEN TRANSKRİPSYONEL REGÜLASYON AĞLARININ BELİRLENMESİ

Perihan Yağmur Güneri Sözeri, İzmir Uluslararası Biyotıp ve Genom Enstitüsü

ÖZET

Mesane kanseri histopatolojik olarak kasa invasiv olan (MIBC) ve kasa invaziv olmayan (NMIBC) mesane kanseri olarak ikiye ayrılır. Hastalık seyri ve tedavi seçenekleri bu iki türde birbirinden çok farklıdır. Bu tez çalışmasında amaç, MIBC ve NMIBC mesane kanseri hücre hatlarını karakterize eden gen regülasyon mekanizmalarını belirlemektir.

H3K27ac kromatin immünopresipitasyonu takiben dizileme (ChIP-Seq) tekniği uygulanarak MIBC(5637, HT1376, J82, T24) ve NMIBC (RT112, RT4) gruplarına özgü enhancer bölgeleri belirlenmiştir. Takiben, bu bölgeler üzerinde bulunan transkripsiyon faktörleri ve muhtemel hedef genleri belirlenmiştir. Kromatin ilişkili proteinlerin seçici izolasyonu (ChIP-SICAP) methodu ile belirlenen transkripsiyon faktörleri ile beraber bulunan proteinler belirlenmiştir. FLI1 and FRA1 ChIP-Seq deneyleri de yapılarak hedef genleri filtrelenmiştir. Son olarak, FLI1 ve FRA1 genleri susturularak hedef genler üzerinde etkisi incelenmiştir.

FLI1 ve FRA1 transkripsiyon faktörleri motifleri MIBC grubuna özgü enhancer bölgelerinde; GRHL2, Tp63 and PPARɣ transkripsiyon faktörleri motifleri NMIBC'ye özgü enhancer bölgelerinde bulunmuştur. MIBC grubuna özgü bulunan hedef genler genellikle "epitel hücre göçü" ile alakalı iken NMIBC grubunun hedef genlerinin çoğunlukla transkripsiyon faktörlerinden oluştuğu gözlemlenmiştir. FLI1 ve FRA1 ChIP-SICAP ve ChIP-Seq deneyleri ve FLI1 ve FRA1 genlerinin susturulmasından sonra, MAP4K4 ve FLOT1 genlerinin bu transkripsiyon faktörleri tarafından regule edildiğini göstermiştir.

Elde edilen bulgular MIBC ve NMIBC gruplarını karakterize eden regülasyon mekanizmalarını ortaya çıkarmıştır. FRA1 ve FLI1, invaziv karakteri regüle eden iki anahtar gen olarak belirlenmiştir.

Anahtar Sözcükler: Mesane kanseri, epigenetik, gen regülasyonu, invazyon

1. INTRODUCTION AND THE AIM

Mutations in chromatin modifier genes can readjust chromatin states. Mutation rate in chromatin modifier genes in bladder cancer is especially high (~20-25%) compared to many other cancer types. When it is considered that around 200.000 people die because of bladder cancer, it is one of the major cancer types for which chromatin regulatory mechanisms should be studied. Once transcriptional regulation networks specific to MIBC and NMIBC are identified, new molecular targets can be introduced to drug industry. In this project, we aim to investigate the transcriptional regulatory networks differentially regulated between muscle invasive bladder cancer (MIBC) and non-muscle invasive bladder cancer (NMIBC) cell lines via identifying the active chromatin regions and transcription factors and their interacting partners specific to the respective cell lines.

2. GENERAL INFORMATION

2.1. Epigenetic Mechanisms and Epigenetics of Cancer

2.1.1. Epigenetics and Mechanisms Involved In Epigenetic Regulation

Conrad Waddington defined the term “epigenotype” in 1942 (1). He was an expert in embryology and developmental biology and he shared his observations on Drosophila Melanogaster and define epigenetics as the dynamic changes between genotype and phenotype driving developmental processes (1). Another definition of epigenetics is that without any difference in the sequence of DNA, the gene(s) function can change, and this change is referred as epigenetic changes (2). Epigenetic mechanisms are thought be heritable like genetics and have impacts on phenotype (3) . Among epigenetic regulations, chemical modifications of histones, and histone variants are regarded as major mechanisms implicated in gene regulation (4). A representative is shown in Figure 1 which basically defines open and closed chromatin regions (5).

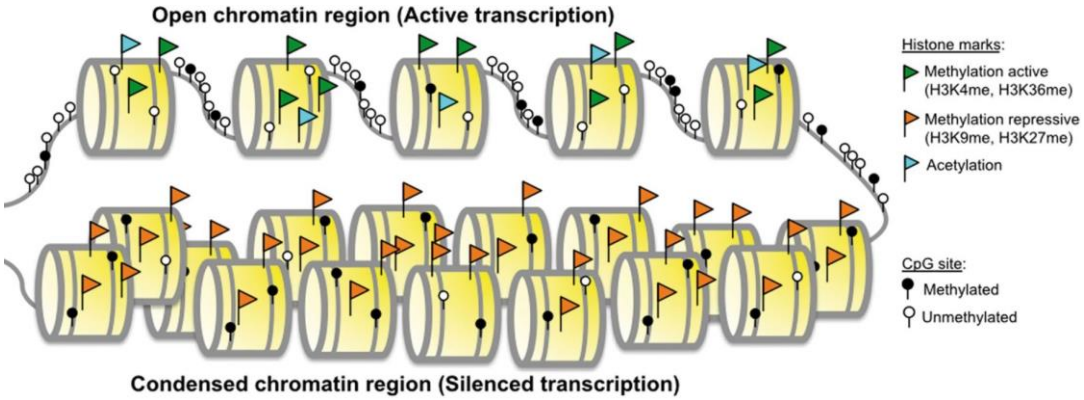

Figure 1. Open and closed chromatin regions with histone marks and methylated or unmethylated CpG sites. This figure is adopted from Kagohara et al. (5).

2.1.2. Epigenetics of Cancer

Cancer is a lethal disease caused by cooperation of many hallmarks (6). These hallmarks are being constantly in proliferative state, blocking the apoptosis, emerging angiogenesis, avoiding from the senescence, being blind for growth suppressors and gaining the ability of metastasis and invasion, re-regulating the metabolism and energetics, escaping from immune system, cellular replicative immortality and instability of the genome (6). Among the collection of activating mutations on proto-oncogenes or de-activating mutations on tumour suppressive genes; epigenetic misregulations also result in over-expression or downregulation of the genes implicated in cancer. Thus, change in epigenetic regulatory mechanisms is also recognized as a major driver hallmark of cancer (7) (8). Basically, change in epigenetic balance throughout epigenome may lead to permissive or restrictive chromatin states, resulting in overexpression of some genes while causing repression of some others (7). These epigenetic deregulatory mechanisms may change from one cancer type to another cancer type but the important point is that the discovery of misregulated regions of the genome which differs between normal cell and cancer cell or invasive cell and non-invasive cell may provide fundamental insights about regulatory mechanisms determining the fate of the cell and enable identification of novel therapeutic targets.

2.1.3. H3K27ac Modification As A Footprint of Active Regulatory Regions

Chemical modifications present on the N-terminal tails of the histones directly affect the three dimensional organization of the genome. There are several histone modifications which play crucial roles in chromatin conformation, important for the regulation of gene expression (9). Acetylation of the 27th Lysine residue on H3 histone (H3K27ac) is one of the histone marks deposited by the acetyltransferase CBP (10). With this acetylation mark, interaction of histones with DNA weakens. Thus, genomic regions marked by H3K27ac becomes more accessible to RNA Polymerase II and transcription factor binding, ideal for robust transcriptional activity (11). In the light of all of these knowledge, H3K27ac is thought as a marker of active regulatory regions. In murine embryonic stem cells, it was shown that H3K27ac mark can differentiate active enhancers from inactive ones and the regions marked by H3K27ac may vary from stage to stage throughout the development (12). All in all, H3K27ac is a surrogate marker of active regulatory regions, reflecting the footprint of the transcription factors specific for different cell types and involved in cell fate decisions.

2.2. Epigenetic Analysis Techniques

2.2.1. Chromatin Immunoprecipitation Followed by Sequencing (ChIP-Seq)

ChIP-Seq is a highly powerful technique which can generate high-throughput data, enabling researchers to examine the genomic regions for localization of histone marks and binding of transcription factors of interest. This technique has been used widely since first paper published in 2007 (13). ChIP-Seq can be used to identify chromatin regions that are enriched by a protein or certain histone marks. This technique basically relies on crosslinking of proteins in chromatin and DNA together, which is followed by the lyses of the cells. Then, chromatin is fragmented and region of interest is captured by antibody-bead coupling. Chromatin fragments including region of interest are then separated from proteins around. After purification

of genomic DNA, it is ready to be sequenced once the sequencing libraries are prepared (14) .

2.2.2. Selective Isolation of Chromatin Associated Proteins (ChIP-SICAP)

Genomic DNA occupied by certain histone modifications or transcription factors of interest can be identified using ChIP-Seq technique. However, the transcriptional regulatory complexes and epigenetic modifiers on target chromatin regions cannot be identified using ChIP-seq only. Chromatin Immunoprecipitation Followed by Selective Isolation of Chromatin Associated Proteins (ChIP-SICAP) is a recently published, highly selective technique based on capturing proteins on target chromatin regions using a bait protein, which can be a transcription factor of interest as can be seen in Figure 2 (15). With the help of this technique, not only target regulatory regions are identified but also the involved regulatory mechanisms can be uncovered via identification of the transcription factors and chromatin modifiers, which are co-bound with the bait protein used in ChIP-SICAP assay at the respective regulatory regions . There are other techniques similar to ChIP-SICAP like RIME or ChIP-MS yet ChIP-SICAP is the most specific one, selecting chromatin binders with high rates (15).

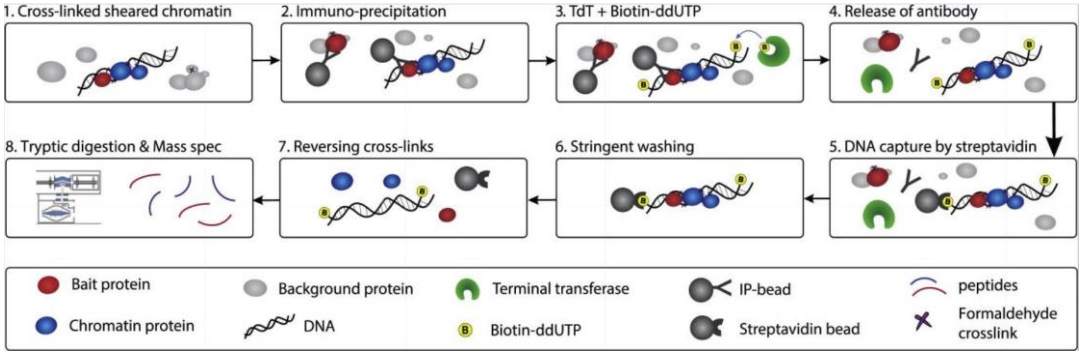

Figure 2. Experimental steps of ChIP-SICAP. This figure is adopted from Rafiee et al. (15).

2.3. Bladder Cancer

2.3.1. General Information About Bladder Cancer

Bladder cancer is the 10th most commonly diagnosed cancer type with reported mortality rates of 9.5 per among a 100000 men and 3.3 per of a 100000 woman worldwide (16). The most common form of bladder cancer originates from urothelium and urothelial carcinoma has two subtypes histopathologically: non-muscle invasive bladder cancer (NMIBC) and muscle invasive bladder cancer (MIBC). The major difference between the two is that while non-muscle invasive bladder cancer does not invade through muscularis propria while muscle invasive bladder cancer does (17). Even if MIBC is much more lethal than NMIBC due to distant organ metastasis followed after invasion to muscle, NMIBC has high recurrence rate, lowering the life quality of the patients and some of NMIBC can progress to an invasive form. As it might be expected, NMIBC and MIBC differ from each other when the genetic alterations are considered. While *TP53* (32%), *KDM6A* (38%), *ARID1A* (24%) and *PIK3CA* (21%), *EP300* (12%) are the top five frequently mutated genes in MIBC as can be seen from Figure 3 (18) NMIBC has the highest mutation frequencies for the genes, *CDKN2A* (42%), *FGFR3* (34%), *PIK3CA* (25%), *KDM6A* (18%) and *KMT2D* (12%), respectively (19) however there is another research reported the mutation rates as FGFR3 (79%), PIK3CA (54%), KDM6A (52%), STAG2 (37%) and KMT2D (30%) (20). Unfortunately, despite this detailed genomic characterization of both NMIBC and MIBC, the mechanisms behind invasion to the muscle are not completely understood yet.

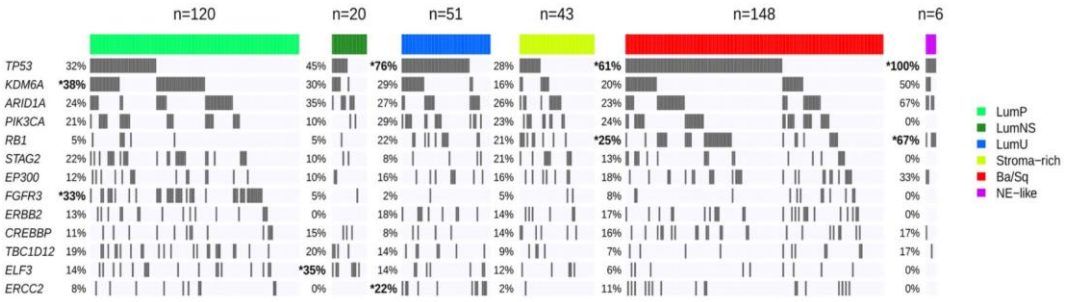

Figure 3. Mutational landscape of MIBC tissue samples. *Figure is adopted from Kamoun et al.(18).*

2.3.2. Epigenetic Misregulations In Bladder Cancer

Mutational landscapes of both NMIBC and MIBC (18-21) show that many of the chromatin modifiers are mutated in bladder cancer. Based on this finding, it is not surprising that bladder cancer is actually considered as a disease of chromatin. Thus, examining the changes in chromatin modifications is essential for identification of new targets in bladder cancer (22). Epigenetic misregulations in bladder cancer point out to the usage of epigenetic inhibitors as good treatment options for bladder cancer (23). In fact, there are several ongoing clinical trials focusing on epigenetic inhibitors like EZH2 inhibitor Tazemetostat or an HDAC inhibitor Mocetinostat in bladder cancer (24). Additionally, as epigenetic mechanisms are highly implicated in metabolic processes (25), epigenetic misregulations in bladder cancer are also recognized as the cause of changes in metabolic pathways like PI3K-Akt pathway (26).

2.3.3. Invasion to Muscle In Bladder Cancer

Mortality rate in bladder cancer has a sharp increase when the disease invade through muscle. When we take a look to the definition of invasion itself, it is a still an issue of heated discussions. From a biological perspective, it is defined as a highly rapid movement of a population from a place to another and become dominant in this new location when there is a disruption in the mechanisms controlling proliferation (27). Invasion mechanism of bladder cancer is still not known (28) however there is some

research focusing on molecular mechanisms that can promote or inhibit invasion ability of bladder cancer. In a study, it was shown that Autophagy Related Gene 7 (*ATG7*) was upregulated in invasive bladder cancer cell lines, tissues and mouse with invasive bladder cancer and downregulation of *ATG7* inhibited invasion of bladder cancer (29). Another study suggested that there is a crosstalk between muscle invasive bladder cancer cells and fibroblasts, which regulates differentiation and invasion of bladder cancer in patients and the mechanism behind is hormonal dysregulations and Hypoxia Growth Factor (*HGF)(30)*. PI_3K-Akt pathway is also found to be highly active in invasive bladder cancer cell lines and bladder tumour samples due to *B7-H3* overexpression; knockdown of *B7-H3* resulted in decrease in the invasion of bladder cancer cell lines (31). *TRIM59* is another gene that is reported to lead an increase in the invasion capacity of bladder cancer cell lines by manipulation of TGFB-Smad2-3 pathway (32). It is also reported that knockdown of *Nodal* gene resulted in decrease in proliferation, invasion and migration via blocking ALK-SMAD pathway (33). *MMP7* is another identified protein promoting invasion of a set of bladder cancer cell lines (34). *FRA1,* a transcription factor from ETS family, is another gene identified positively regulating invasion of bladder cancer cell lines (35). All in all, there are reported genes that regulate the invasion of bladder cancer. However, the genomic and epigenomic mechanisms driving the invasion still need to be uncovered.

2.3.4. Treatment of NMIBC and MIBC

As mentioned above, NMIBC and MIBC have different molecular characteristics. Because of this, distinct treatment options are preferred in clinic. The treatment of NMIBC mostly relies on TURBT followed by Bacillus Calmette-Guerin (BCG) treatment yet, this has strong side effects (36). Besides, there are also NMIBC patients who are unresponsive to BCG treatment. These patients have better response to Pembrolizumab but still there is a need for new therapy options which have less side effects and which are more effective (37). On the other hand, the treatment of MIBC is

mostly relies on neo-adjuvant chemotherapy which improves survival of the patients like Cisplatin based neo-adjuvant chemotherapy (38) (39). Besides, some group of MIBC patients especially older ones, cannot manage Cisplatin based neo-adjuvant therapy. In this kind of situation, Carboplatin-Gemcitabin based neo-adjuvant chemotherapy can be one of the options (40). Atezolizumab, Nivolumab, Pembrolizumab, Avelumab, Durvalumab are other chemotherapatic options that can be used in Platinum unresponsive or ineligable patients with MIBC (40). Among all these treatment options for both NMIBC and MIBC, there is certainly need of new theraupathic targets that improve patients' quality of life and response to the treatment.

3. MATERIALS AND METHOD

3.1. Type of The Research

Experimental.

3.2. The Place and The Time of Research

Thesis Project was done at Izmir International Biomedicine and Genome Institute and International Izmir Biomedicine and Genome Center between 2018-2021.

3.3. Working Material

This thesis was done using 5637, HT1376, J82, RT112, RT4 and T24 cell lines. RT4 and J82 cell lines were kindly provided by Şerif Şentürk and T24 cell line was provided by Neşe Atabey. 5637, RT112 and HT1376 cell lines were ordered from German Collection of Microorganisms and Cell Cultures GmbH (DSMZ).

3.4. Variables of The Research

H3K27ac mark of the MIBC and NMIBC cell lines are independent variables. Group specific enhancers and transcription factors regulating specific enhancers are dependent variables.

3.5. Tools Used to Obtain Data

3.5.1. Materials

3.5.1.1. Equipment

Equipment used in this thesis were listed in Table 1.

Table 1. Equipment used in this thesis.

Equipment	Company
Micropipettes	2 µl, 10 µl, 20 µl, 200 µl, 1000 µl Gilson
Microcentrifuge	Thermo Scientific Micro CL 17R 230 V.
PowerPac™ Basic Power Supply	Bio Rad
Mini Electrphoresis System	Thermo Scientific OWL B1A
Centrifuges	Eppendorf, Beckman
Human Cell Culture Incubator	memmert
Nanodrop	Thermo Scientific NanoDrop 2000
Class II Biological Safety Cabinets	Thermo Scientific SAFE 2200
Sonicator	Covaris S220
Water Tank	Nuve NB9
Light Microscope	ZEISS Vert.A1
Hemocytometer	ISOLAB
Ice Machine	HOSHIZAKI
Freezer (-20)	Bosch - GSN 51 AW
Nitrogen Tank	CHART
Microplate Spectrophotometer	MULTISCAN GO, Thermo Scientific
Freezer (-80)	Newsburck
Western Blot System	BIO-RAD
Electronic pipettor	ISOLAB, Gilson

Fume Hood	Kötterman 2-401-GAAAAY
Thermal Cycler	Simpleamp A24811
Real Time PCR System	ABI 7500 Fast
Mini Vortex Mixer	Thermo Scientific ELED-88880018/ LPMixer
Tube Rotator	Thermo Scientific Eled 88881002
Micro Centrifuge	Thermo Scientific TS-75004061 mySPIN
Lab Scale	Sartorious ENTRIS 822-1S Model
Volume Measuring Equipments	ISOLAB
Magnetic stirrer	Thermo Barnstead / BS-SP131320-33Q
pH meter	Hanna ELED Model
Erlens	ISOLAB
Cool Rack	Corning
Mr. Frosty Freezing Container	Thermo
Washing Bottles	ISOLAB
Borosilicate glass bottles	ISOLAB
Spray bottles	ISOLAB
Spatula set	ISOLAB
DYNAL DynaMag Dynabeads DynaMag 2 Magnet	Thermo Fisher Scientific
Cell culture dishes	Corning
Cryogenic tubes	Corning
Cell scrapers	ISOLAB
MicroAmp™ Fast Optical 96-Well Reaction Plate	Thermo Fisher Scientific
Multiwell plates	Corning
Vacuum filtration system	Milipore

Falcons (15ml, 50ml)	SPL
PCR tubes	Neptune
Examination Gloves	ISOLAB
Serological Pipettes	SPL
Eppendorf tubes (0.5ml, 1.5ml, 2ml)	Thermo Fisher Scientific
Disposable pipette tips	Neptune
Nitrocellulose membrane	BIO-RAD
Color Prestained Protein Standard	NEB P7719S
Glass Pasteur Pipette	ISOLAB
DNA LoBind Tube (1.5 ml)	Eppendorf
Shaker	Thermo Scientific
LI-COR	ODEYSSEY CLx
Bioruptor Pico Sonicator	Diagenode

3.5.1.2. Chemicals

Chemicals used in this thesis were listed in Table 2.

Table 2. Chemicals used in this thesis.

Chemical	Company
EDTA	Sigma-Aldrich
Ethanol	Merck
Methanol	Sigma-Aldrich
NaCl	Sigma-Aldrich
Glycerol	Sigma-Aldrich
Phosphate Buffer Saline (10X)	Thermo Fisher
TritonX-100	Sigma-Aldrich
Na deoxycholate	Sigma-Aldrich
SDS	Invitrogen
Tris	Sigma-Aldrich

EGTA	Sigma-Aldrich
Protease inhibitor coctail	Roche
Glycine	Sigma-Aldrich
HCl	Sigma-Aldrich
Tween-20	Sigma-Aldrich
Ponceau	Sigma-Aldrich
Acetic Acid	Sigma-Aldrich
Formaldehyde	Sigma-Aldrich
Tris Acetate-EDTA (TAE) Buffer (10X)	Sigma-Aldrich
Agarose	Sigma-Aldrich
Isopropanol	Sigma-Aldrich
B-mercaptoethanol	Sigma-Aldrich
Bromophenol blue	Sigma-Aldrich
TEMED	Sigma-Aldrich
10% APS	Biofroxx
Protogel	National Diagnostics
Skim milk powder	Sigma-Aldrich
$NaHCO_3$	Sigma-Aldrich
LiCl	Sigma-Aldrich
TERGITOL™ NP-40 (70%)	Sigma-Aldrich
DOC	Sigma-Aldrich
Protogel Stacking Buffer	National Diagnostics

3.5.1.3. Buffers

Buffers used in this thesis were listed in Table 3.

Table 3. Buffers used in this thesis.

Name of the Buffer	
Elution Buffer (0.5 ml) (ChIP)	
Component	**Amount**
10% SDS	50 µL

1 M $NaHCO_3$	50 µL
dH_2O	400 µL
DOC buffer : 2ml (ChIP)	
Component	**Amount**
1 M Tris pH 8	20 µL
1 M LiCl	0.5 mL
NP-40	10 µL
DOC (%10)	0.1 mL
0,5 M EDTA	4 µL
dH_2O	1366 µL
ParoFix : 50ml (ChIP)	
Component	**Amount**
0.1 M Hepes pH 8.0 (NaOH)	50 µL
0.5 M EDTA	200 µL
0.1 M EGTA	500 µL
5 M NaCl	2 mL
11% formaldehyde (add fresh before use)	
Paro Rinse 1 : 500ml (ChIP)	
Component	**Amount**
1 M Tris pH 8.0	5 mL
0.5 M EDTA	10 mL
0.5 M EGTA	0.5 mL
Triton X-100	1.25 mL
dH_2O	483 mL
Paro Rinse 2 : 500ml (ChIP)	
Component	**Amount**

1 M Tris pH 8.0	5 mL
0.5 M EDTA	1 mL
0.5 M EGTA	0.5 mL
NaCl	20 mL
dH_2O	473 mL
Lysis Buffer : 500ml (ChIP)	
Component	**Amount**
1 M HEPES/KOH pH 7.5	25 mL
5 M NaCl	50 mL
0.5 M EDTA	1 mL
%100 Triton X-100	5 mL
%10 DOC	5 mL
%20 SDS	2.5 mL
dH_2O	411.5 mL
Add fresh: protease inhibitors	
RIPA Buffer (1X/50 mL)	
Component	**Amount**
Triton X-100 (10%)	5 mL
Na deoxycholate (10%)	2,25 mL
SDS (20%)	250 µL
Tris-Cl pH 7,4 (1M)	2,5 mL
NaCl (5M)	1,5 mL
EDTA pH 8 (0,5M)	100 µL
EGTA (0,1M)	500 µL
Protease Inhibitor Coctail (for 1 mL)	40 µL
Running Buffer (10X/1L) pH~8,3	
Component	**Amount**
250 mM Tris base	30.2 g

1,9 M Glycine	142 g
1% SDS	
Transfer Buffer (10X/1L) pH~8,3	
Component	**Amount**
250 mM Tris base	30.2 g
1,9 M Glycine	142 g
20% Methanol (add before use)	200 mL
TBS (10X/1L) pH~7,6	
Component	**Amount**
Trizma HCl	24.23 g
NaCl	80.06 g
TBST (1X/1L)	
Component	**Amount**
TBS (10X)	100 mL
dH_2O	900 mL
Tween-20	1 mL
Ponceau Dye	
Component	**Amount**
Acetic Acid	0.5 mL
Ponceau	0.25 mL
dH_2O	50 mL
Laemmli Buffer	
Component	**Amount**
0,5 M Tris-HCl (pH=6,8)	20 mL
Glycerol	20 g
SDS	4 g

Bromphenol Blue	0,05 g
1 M DTT	2 mL
dH_2O	13 mL
IP Buffer (ChIP-SICAP)	
Component	**Final Concentration**
Tris-HCl pH 7.5	50 mM
Triton X-100	1%
NP-40	0.5%
EDTA	5 mM
Elution Buffer (ChIP-SICAP)	**Final Concentration**
SDS	7.5%
DTT	200 mM
SDS Washing Buffer (ChIP-SICAP)	**Final Concentration**
Tris-HCl pH 8	10 mM
SDS	1%
NaCl	200 mM
EDTA	1 mM
BW2x Buffer (ChIP-SICAP)	**Final Concentration**
Tris-HCl pH 8	10 mM
Triton X-100	0.1%
NaCl	2 M
EDTA	1 mM
LB3 Buffer (ChIP-SICAP)	**Final Concentration**
Tris-HCl pH 8	10 mM
NaCl	100 mM
EDTA	1 mM

EGTA	0.5 mM
Na-deoxycholate	0.1%
N-lauroylsarcosine	0.5%

3.5.1.4. Kits

Kits used in this thesis were listed in Table 4.

Table 4. Kits used in this thesis.

Kit	**Company**
Pierce™ BCA Protein Assay Reagent Assay	ThermoFisher Scientific
FastStart Essential DNA Green Master	Roche
DNA Clean & Concentrator	Zymo Research
Lipofectamine 3000 Reagent	ThermoFisher Scientific
MAXIMA First Strand cDNA Synthesis Kit	ThermoFisher Scientific
NucleoSpin RNA, Mini kit for RNA purification	MACHEREY-NAGEL
Taqman Universal MMIX II NO UNG 5ml	Thermo Fisher Scientific

3.5.1.5. Cell Culture

Cell culture ingredients used in this thesis were listed in Table 5.

Table 5. Cell culture ingredients used in this thesis.

Solutions	**Company**
Roswell Park Memorial Institute (RPMI) Medium	Gibco
Fetal Bovine Serum (FBS)	Thermo Fisher Scientific 10500064
Penicillin/Streptomycin	Thermo Fisher Scientific 15140122

Gibco Trypan Blue	Thermo Fisher Scientific 15-250-061
Freezing Medium	Thermo Fisher Scientific 12648010
Phosphate-Buffered Saline (PBS)	Thermo Fisher Scientific 70011036
TrypLE	Thermo Fisher Scientific 12604013
Opti-MEM	Thermo Fisher Scientific 31985062
DMEM, high glucose	Gibco 41965039

3.5.1.6. Antibodies

Antibodies used in this thesis were listed in Table 6.

Table 6. Antibodies used in this thesis.

Antibody	**Company**	**Cat. No.**
Anti-rabbit IgG (H+L) (DyLight™ 800 4X PEG Conjugate)	Cell Signaling Technology	5151S
IRDye® 680LT Donkey (polyclonal) anti-Mouse IgG Secondary Antibody (H+L)	Li-COR	926-68022
β-Actin (8H10D10) Mouse mAb	Cell Signaling Technology	#3700
FRA1 Rabbit Monoclonal Antibody	Cell Signaling Technology	#5281
Anti-FLI1 Antibody	Abcam	ab15289
H3K27ac Antibody	Active Motif	39133

3.5.2. Wet Lab Experiments

3.5.2.1. Cell Line Maintenance

Cell lines used in this thesis were maintained at 37 °C with 95% humidity and 5% CO_2. 5637 and RT112 cell lines were maintained using RPMI-1640 Medium supplemented with 10% FBS and 1% Penicillin while HT1376, J82, RT4 and T24 cell lines have been grown in Dulbecco's Modified Eagle Medium (high glucose) supplemented with 10% FBS and 1% Penicillin.

3.5.2.2. Chromatin Immunoprecipitation

Schubeler Lab ChIP protocol was modified a little and used as chromatin immunoprecipitation (ChIP) protocol (41). 15-20 million cells were used per ChIP experiment. H3K27ac ChIP assay was performed with 5637, HT1376, J82, RT112, RT4 and T24 cell lines and FRA1 and FLI1 ChIP were performed with T24 cell lines. First cells were crosslinked with %1 formaldehyde for 10 minutes (RT) for H3K27ac ChIP experiments and 1.25% formaldehyde for 15 minutes (RT) for FRA1 ChIP experiments. Crosslinking was stopped by addition of 2.5 M (final concentration) Glycine for 10 minutes at +4 °C. After this step, cells were washed and then lysed with Lysis Buffer and 1X Protease Inhibitor Cocktail (Roche, 11873580001). In order to perform immunoprecipitation efficiently, chromatin was fragmented into small pieces (200-600 base pairs) by using S220 Covaris Ultrasound Sonicator. Optimized sonication cycles for each cell line determined to be different and the range is between 5 cycles to 30 cycles. After sonication of the chromatin samples, 50 µL was taken for input fraction and the rest is used for IP. For input fraction, reversal of crosslinking protocol was applied. Reversal of crosslinking protocol begins with addition of 150 µL TE buffer and of 4 µL RNase (10mg/mL) to the input chromatin and incubation for 30 minutes at 37 °C, followed by 1% SDS (final concentration),100 mM NaCl (fc.) and 2 µL Proteinase K (20mg/mL) addition and incubation at 55 °C for at

least 2.5 hours then overnight incubation at 65 °C. Zymo DNA Clean-up & Concentrator Kit was used to purify genomic DNA.

To perform the IP step, was continued with the addition 4 µg H3K27ac antibody (Active Motif, 39133) to 40 µL Dynabeads M280 Anti Rabbit Magnetic beads (Thermo Fisher, 11204D) (pre-washed with BSA) and rotating overnight at +4 °C for H3K27ac ChIP. 950 µL chromatin remained after sonication was then bound with pre-washed magnetic beads coupled with H3K27ac antibody for 3 hours. After that, stringent washes were done using a freshly prepared DOC buffer, Lysis buffer and TE. Immunoprecipitated chromatin was then eluted by resuspending the beads in a freshly prepared 100 µL elution buffer by agitating the sample at 1000 rpm at 25 °C for 15 minutes, and centrifuging the sample at 11000 rpm for 2 minutes at room temperature. Elution step was repeated once more. Then, reversal of crosslinking for ChIP fraction is started with the incubation of ChIP chromatin with 4 µL RNAse (10 mg/mL) at 37 °C for 30 minutes and followed by the addition of 4 µL 0.5 M EDTA, 8 µL of 1M Tris (pH=6.5) and 0.5 µL Proteinase K (20 mg/mL) and incubation at 55 °C for at least 2.5 hours. Lastly overnight incubation at 65 °C was done. ChIP DNA was purified by using Zymo DNA clean-up & concentrator kit. For the transcription factor ChIP experiments (FRA1 and FLI1), a slightly more stringent protocol was applied. Before IP, chromatin was precleared by addition of 10 µL of pre-blocked magnetic beads (blocked with 10 µL tRNA (10 mg/mL) and 10 µL BSA (10 mg/mL) and rotating the sample at +4 °C for 1 hour. After chromatin pre-clearing, antibodies targeting transcription factors (FRA1 and FLI1) were added to the chromatin sample with 1:100 dilution and the sample is rotated overnight at +4 °C. Following day, antibody-coupled chromatin was coupled with 50 µL pre-blocked magnetic beads by rotating at +4 °C for 3 hours. All other steps were done in the same manner as in H3K27ac ChIP experiments.

3.5.2.3. Agarose Gel Electrophoresis

Size of the chromatin fragments were checked using agarose gel electrophoresis. 1.7% Agarose gels were prepared with Tris-Borate-EDTA buffer and 2 µL of Safe-view Classic Nucleic Acid Stain was added when the gels were in physiological temperature. Then gels were immediately placed on the loading tank and waited to get polymerized. When the gels were polymerized, input DNA of ChIP samples were prepared to be loaded on agarose gels. Orange DNA Loading Dye (NEB) was added to input DNA and also 100 base pairs (bp) and one kilo base (kb) DNA ladders (1X final concentration) were added. Once the samples were loaded on gels, DNA was run at 100 V for ~40 minutes.

3.5.2.4. ChIP-qPCR

For H3K27ac ChIP validation, Taqman Universal MMIX II NO UNG were used with final 2.5 µM primer concentrations and reactions were run on Applied Biosystems 7500 Fast Real Time PCR. Sample running conditions for Taq-Man Kit was: 95 °C for 15 minutes, 95 °C for 15 seconds and 60°C for one minute for 40 cycles. On the other hand, FastStart Essential DNA Green Master Kit were used for FRA1 and FLI1 ChIP validation. In each ChIP-qPCR experiment, ChIP DNA was diluted in 1:2 ratio while input DNA was diluted to 1:10 ratio. Primers and probes (if it is needed) used in ChIP-qPCR experiments were listed below in Table 7. Enrichment of the chip was calculated using “input%” method (42).

Table 7. Primers and probes used in ChIP-qPCR experiments for the validation of H3K27ac ChIP. Positive control regions are highlighted with green while negative ones are labelled with red. While MCL1, ATRAID and RARA were used as positive control regions; NCT1, NCT2 and GABRA2 were used as negative control regions of FRA1 ChIP experiments. YWHAZ and ATRAID regions were used as positive control regions of FLI1 ChIP and NCT1, NCT2 and ENHR2 were used as negative control regions.

Gene Name	Forward Primer	Reverse Primer	Roche Probe No
DLGAP1	tggagtcttgtgcctaagtgc	agggaaatggcagaaatgg	12
ELF4B	cagtaatggtagactctggcttga	cggtgattcacgtctacgaa	12
MCL1	aatgaacccccttaccttgg	aagccaatgggcaggtct	4
DDIT4	cctttgggaccgcttctc	atctggggtgggagttcg	10
YWHAZ	cgtctctaagggaccgacag	ggtgagcctgagcatagcc	49
ROCK1	cccgatggagacttagcaga	ccaactatcgtcttcctcttcg	19
TGIF1	gactcgggacagggaattg	gcgcgtgtctctagacctgt	14
LZTS2	ctgaggctgagagcgtgtc	gcagctggtcattgttcca	70
ATRAID	gctacccgaggtacagaagc	agcgtcagggacgaaatcag	NA
RARA	ggtaaagtttcagcctccgc	cacagcgtctgccctaacc	NA
SOX10	ccagggaacctgggactc	ctggagctgagcactctgg	4

PRAC1	tggtctggaactcctgtgct	aacatctactgggcgagacc	4
GABRA2	ttttcttcactccccttaacaaa	gacttggtcttgggcaacc	4
DEDD2	aatcccagctactggggaag	cactgcagcctccagctc	2
EMBP1	cagtaggagctctttgttttggt	gcccagagactcctgagttaaa	48
GLIS2	aaaaacagatgtgttacccctca	tctcccctagagccttccag	19
Negative control 1	gaccactggcgatctcacta	ggtagtagcttcagtggagaagt	NA
Negative control 2	ggtgagatggattggtaagaccc	aaagccagatttgaccaagca	NA
Enhancer Region 2	tgtggccttgcctcaactatg	ggttattgcatttgggcaggat	NA

3.5.2.5. ChIP-SICAP

ChIP part of the protocol was started with crosslinking T24 cell line (15-20 million cells per experiment) with 1.5% final concentration of formaldehyde for 15 min and followed by addition of 150 mM (fc.) Glycine for 5 minutes, continuously shaking at RT. After a couple of washing and lysing steps, protein concentrations were measured in the presence of 1 % PBS-SDS. Standard proteins were treated the same except Benzonase addition. Samples were incubated at 95 °C for 5 minutes. Then T24 chromatin's DNA and proteins were separated by adding 0.5 µL Benzonase (Sigma Aldrich, E8263-5KU) and vortexing. 25 µL from prepared samples were added to one well of 96 well plate and Pierce™ BCA Protein Assay Kit manual was followed to measure the protein content. Overall, for each replicate, chromatin samples corresponding to nearly 2 µg protein were used for ChIP assays performed for FRA1 and FLI1 transcription factors. Each chromatin sample was sonicated for 19 cycles, 1 minute on/1 minute off on Covaris S220. Input DNA of each sample was controlled for sonication size. After sonication, the samples

were centrifuged for 10 minutes at 12000 g at +4 °C. TritonX-100 was added to the supernatants with a final concentration of 1.5%. Then FLI1 (1:50 dilution) and FRA1 (1:50 dilution) antibodies were added to the samples and antibodies were coupled with chromatin samples overnight at +4 °C cold room with 800 rpm agitation on Thermomixer. Chromatin samples not bound with antibody were used as negative controls. Next day, the samples were centrifuged at +4 °C for 10 minutes at 12000 g. Supernatants were taken and filled up to 1 mL with IP Buffer. Meanwhile, 50 µL Dynabeads (M280 Anti Rabbit Magnetic Beads) for each sample were washed with IP Buffer (+4 °C) once. Pre-washed magnetic beads were then added to the samples and coupled at +4 °C for 3 hours by rotating. Then samples were washed and resuspended with 200 µL PBS-T (PBS including 0.1% Tween20) and shipped to Francis Crick Institute for the SICAP part of the protocol. In there, SICAP protocol was followed as already described (15, 43). Klenow 3'-exo minus, T4 PNK, and dNTPs (NEB) treatments were applied to the beads. Then the beads were biotinylated with terminal deoxynucleotidyl transferase (TdT (Thermo Fisher)) and 1:1 ddUTP and dCTP. After that the beads were washed with IP buffer 6 times and proteins were eluted by adding elution buffer and waiting for 15 minutes at 37 °C. Then the samples were diluted in IP buffer and 100 µL of pre-resistant streptavidin beads were added on the samples. After an incubation in room temperature for 1 hours by rotating the samples, stringent washes were done 3 times with SDS Wash buffer, once with BW2x, once with 20% isopropanol and once with 40% acetonitrile in water. Then the tubes were transferred to PCR tubes, put on magnetic stand and supernatant was discarded. 15 µL Ambic 50mM plus DTT 10mM final concentration was used to resuspend the beads and the samples were incubated at 50 °C for 15 minutes. Then alkylation was performed with the addition of IAA with 20 mM final concentration and incubated for 15 minutes in dark. 10 mM DTT addition was followed the alkylation and 300 ng LysC (Wako) was added to samples for the digestion of the proteins and samples were incubated overnight at 37 °C.

After the incubation, beads were collected on magnetic stand and supernatant of the samples were taken. 200 ng Trypsin (Promega, V5280) was then added to each sample and samples were incubated for 6-8 hours at 37 °C. After final incubation, peptide clean-up was performed using Ziptips with 0.6 µL C18resin (Merck).

3.5.2.6. Knockdown Experiments

Knockdown of FLI1 and FRA1 genes was performed by using –UU tagged custom siRNA targeting the region 5'-CACCAUGAGUGGCAGUCAG-3' and 5′-GUUCACUGCUGGCCUAUAA-3' for the knockdown of FRA1 (44) and FLI1 (45), respectively. These custom siRNA oligo nucleotides were ordered from GE Healthcare Dharmacon, Inc. MISSION® siRNA Universal Negative Control (SIC001) was used as negative control for knockdown experiments. For unique knockdowns, 75 nM siRNA per knockdown was transfected when the cells were approximately 80% confluent using Thermo Fisher Lipofectamine 3000 Transfection Reagent according to manufacturer's protocol. On the other hand, double knockdown experiments (both FLI1 and FRA1 siRNA used) were performed by using 50 nM siRNA constructs from each siRNA.

3.5.2.7. Protein Isolation

Protein isolation was done by scraping the cells from the plate with the help of 200 µL RIPA+PIC buffer. Lysed cells were then immediately vortexed vigorously and incubated on ice for 10 minutes. This step is repeated for 3 times and then samples were sonicated for 5 cycles (30 seconds on/30 seconds off) on BioRuptor Pico Sonicator. After that samples were centrifuged at 17000 g for 20 minutes at +4 °C. Lastly, supernatant of centrifuged samples which includes proteins were taken to new tubes and stored at -80 °C.

3.5.2.8. BCA Protein Assay

Concentrations of the protein samples were measured using Thermo Fisher's BCA Assay Kit. 2 mg/mL protein standard present in the kit was serially diluted with RIPA + PIC to 1, 0.5, 0.25, 0.125, 0.0625, 0.03125 mg/mL. Then, master mix consisting of Buffer A and Buffer B (1X final concentration) inside the kit were prepared considering that 50 µL of master mix is going to be used per well (96 well plate). 2 µL of proteins was also added to wells to measure the concentration of the proteins. MULTISCAN GO (Thermo Fisher) was used to measure the concentration of the proteins at 562 nm wavelength**.**

3.5.2.9. Western Blot

Before running the Western Blot experiment, the concentrations of the proteins were equalized. Protein samples were diluted with RIPA + PIC according to the protein concentration of the samples, βmercaptoethanol-Laemli solution was added on samples at 1X final concentration. Then, protein samples were boiled at 95 °C for 5 minutes and stored at -20 °C. 30 µg protein from each protein sample was loaded per well during Western Blot experiments. Firstly, %8 SDS Page Separating Gel was loaded to gel glasses and immediately covered with 60% isopropanol. Once it was polymerized, SDS Page Stacking Gel was added. When the gel was polymerized, the wells of the gel were washed once with distilled water and then placed in Bio-RAD Western-Blotting tank and cold 1X Running buffer, filled until "2-gel" line of the tank. Proteins were run at 90 V until they pass through stacking gel, then they were run at 120 V for approximately one and a half hours. After separating the proteins according to their size, proteins were transferred to nitrocellulose membrane with sandwich technique in freshly methanol added ice cold 1X Transfer Buffer at 350 mA for one and a half hours. When the proteins were transferred to the membrane, transfer status was first checked with Ponceau Dye and then proteins on membrane were blocked with 5% milk powder dissolved in TBS-T for one hour on shaker.

After blocking of the proteins, membrane was washed with TBS-T once and 1:1000 diluted (with 5% milk powder) antibodies targeting FRA1 or FLI1 were added on membranes. Incubation of membranes with antibody was overnight at +4 °C on shaker. Once the antibodies were bound to proteins of interest, membranes were washed with TBS-T for 10 minutes on shaker and this washing step was repeated three times. Then Anti-rabbit IgG (H+L) (DyLight™ 800 4X PEG Conjugate) (1:30000 diluted) was added on membrane and incubated for one hour at RT on shaker. Stringent wash with TBS-T was repeated again for three times as two step before and then first images of the membrane were taken on LI-COR at 800 nm, 169 µm, “auto” adjustments. After that, B-actin antibody with 1:1000 dilution (with 5% milk powder) was added on membrane for one and a half hours on shaker at RT. Three times wash with TBS-T was repeated again. Then 1:15000 diluted IRDye® 680LT Donkey (polyclonal) anti-Mouse IgG Secondary Antibody (H+L) was added on membrane for one hour at RT on shaker. Last wash of the membrane was repeated again with TBS-T every ten minutes for three times. Membranes were then visualized on LI-COR at both 700 and 800 nm, 169 µm and “auto” conditions.

3.5.2.10. RNA Isolation

48 and 72 hours after transfection, RNA samples were collected using MN Nucleospin RNA Isolation Kit. 350 µL of Buffer RA was mixed with 3.5 µL β-mercaptoethanol per sample and cell pellet was dissolved in this mixture by pipetting at least 50 times. Then the samples were placed in violet ring columns and centrifuged for one minute at 11000 g. The samples filtered were then mixed with 350 µL 70% ethanol (MERCK) by pipetting and then taken to a new column (light blue ring). RNA was bound to light blue ring including columns with the help of ethanol and centrifuging for one minute at 11000 g. Then the columns were placed to a new collection tube and 350 µL of MDB solution was added on columns. Then the columns were spinned at 11000 g for one minute. Meanwhile,

DNAse reaction mixture was prepared by mixing 90 µL reaction buffer for rDNase and 10 µL of rDNase per sample. When centrifuge ended, 95 µL from rDNase master mix was added to each column and incubated for 15 minutes at RT. Isolation of RNA continued with a couple of washes. At first, columns were washed with 200 µL RAW2 Buffer and centrifuged at 11000 g for one minute. This wash was followed by addition of 600 µL RA3 Buffer to the columns and centrifuged for one minute at 11000 g. Last wash was performed by adding 250 µL RA3 Buffer and centrifuging for two minutes for this time at 11000 g. After the washing steps, RNA was eluted with 40 µL RNase-free water by centrifuging at 11000 g for one minute. Eluted RNA concentrations were measured using Nanodrop 2000 Device. All RNA samples were stored at -80 °C.

3.5.2.11. RT-qPCR

One µg of each RNA was converted to cDNA by using Maxima First Strand cDNA Synthesis Kit (Thermo Fisher) by following Kit's instructions. After converting RNA to cDNA, FastStart Essential DNA Green Master was used to detect expression levels of target genes of *FLI1* and *FRA1.* cDNA samples were diluted to 1:5 with ultrapure water and then used to check the expression level of the genes. Primers used were listed in Table 8.

Graphs representing the changes in mRNA level were created using GraphPad Prism 8.3.0 (46).

Table 8. Primer sets used after FLI1 and FRA1 knockdown experiments.

Target gene name	**Forward primer**	**Reverse primer**
FLI1	ACCTCCCACACCGACCAAT	GGACTTTTGTTGAGGCCAGAA
FRA1	CTACCCTCAGTACAGCCCCC	TTCCAGTTTGTCAGTCTCCTGTT
MAP4K4	CCGAGCGCGAGAGGTACA	GGGAGAAGGGTCACTGAAGG
FLOT1	TCTCAACACACTGACCCTCAAT	AGGAACATCTGACAGGCGG

3.5.3. Dry Lab Experiments

3.5.3.1. ChIP Library Preparation and Sequencing

Libraries of ChIP and Input DNA were prepared by GeneCore EMBL Team. After library preparation, H3K27ac ChIP samples were sequenced as 50 bp single end reads on Illumina HiSeq 2500 Device and FLI1 and FRA1 ChIP Samples were sequenced as 75 bp single end on Illumina NextSeq 500 high output mode. Library preparation of ChIP-Seq samples was done by EMBL GeneCore team using NEBNext DNA Ultra II Kit.

3.5.3.2. Alignment and Quality Control Analysis

Alignment of the ChIP-Seq reads to GRHg38 was performed by GeneCore EMBL Team. Burrows Wheeler Aligner (BWA) version 0.7.17-r1188 was used for the alignment with default parameters (47). Sequencing quality was controlled using HOMER NGS Data Analysis Tool version 4.10.3. (48). At first reads were tagged by running "–makeTagDirectory" command. After that "tagged" reads were plotted

according to frequencies of the tags by using –boxplot function in R Programming language.

3.5.3.3. Peak Finding

H3K27ac ChIP-Seq peaks were called using MACS2 algorithm's (49) "-callpeak" function with "-g hs" "--broad" and "-f BAM" additional parameters. After finding H3K27ac peaks, peaks contained completely within promoter regions (-/+ 1kb to transcription start site of protein coding genes) defined in GENCODE v30 Comprehensive Gene Annotation Data (50) were excluded from the peak regions. With this method, we focused on the enhancer sites in this thesis. On the other hand, FLI1 and FRA1 ChIP-Seq samples' peak regions were identified using HOMER NGS Data Analysis Tool's "-findPeaks" command with "-style factor" option which is more suitable for finding the peak regions from transcription factor ChIP-Seq data (48).

3.5.3.4. Finding MIBC and NMIBC Specific Peak Regions

Bladder cancer cell lines were grouped according to their ability of invasion through muscle. 5637, HT1376, J82 and T24 cell lines were in muscle invasive bladder cancer group (51-54) while RT112 and RT4 cell lines composed non-muscle invasive bladder cancer cell lines group (51). Group-specific H3K27ac peak regions were defined with the help of DiffBind R Bioconductor Package with default parameters (55). Venn diagrams representing the overlap of active regulatory regions were plotted using "dba.plotVenn" function in Diffbind and correlation heatmaps representing read counts on active regulatory regions were plotted using "plot" function in Diffbind R Package. Valcano plots showing the scatter of the reads on differential active regulatory regions were plotted using "dba.plotVolcano" function in Diffbind R Package.

3.5.3.5. Transcription Factor Motif Finding Analysis

Transcription factor motif finding analysis was done using HOMER NGS Data Analysis Tool. At first, muscle invasive bladder cancer cell lines' tag directories were combined to one tag directory using "-makeTagDirectory" command and same was done for non-muscle invasive bladder cancer cell lines (48). After creating each groups' tag directories, nucleosome free regions were found using "-findPeaks" command with "-nfr" parameter (48). After defining nucleosome free regions that are thought to be bound by transcription factors, these regions were overlapped with group specific enhancer regions using "GenomicRanges" package in R (56) to identify the nucleosome free regions located within group-specific enhancer regions. Then these regions were used to search for transcription factor motifs using HOMER Tool's "findMotifsGenome.pl" with "-size given" option (48).

3.5.3.6. GO Term Analysis

Gene Ontology (GO) Term analysis of the target genes which are protein coding according to GENCODE v30 Comprehensive Gene Annotation data (50) was done using clusterProfiler R Package (57). Enriched GO Terms of identified MIBC target genes were found using "enrichGO" function with p value adjusting with "FDR" method and filtering to GO level 4. Besides, NMIBC target genes' GO Term analysis was done using the same function "enrichGO" with "FDR" p value adjusting method yet maximum gene ontology set size was increased to 3000 (default value is 500). Top 10 enriched GO Term results were visualized using "dotplot" function in the same package.

3.5.3.7. Identifying "Expressed" Gene Targets of MIBC and NMIBC Specific Enhancers

Target genes of defined MIBC and NMIBC specific enhancers (FDR =< 0.05) were predicted using UCSC geneHancer Tool (58, 59) with "GeneHancer Interactions" as output file type. Predicted gene targets

were then filtered according to their mean expressions in cell line groups (NMIBC and MIBC). RPKM normalized expression values of the all protein-coding genes were obtained from Cancer Cell Line Encyclopaedia Database (60). First, genes having “0” value of RPKM were discarded from the RPKM data. Afterwards, rest of the genes were clustered as “not-expressed” and “expressed”. Clusters were created using Gaussian Mixture Modelling using Mclust R Package (61) with “G=3” option. Accordingly, for NMIBC group, genes which have log2(RPKM) value > -0.77 are defined as “expressed” while this cut-off is 0.98 for MIBC group (p value < 0.05). These cut-off values were used to filter the target genes of group-specific enhancers and the target genes defined as “not expressed” were discarded. After this filtration, 456 and 1752 target genes were identified to be regulated by NMIBC-specific enhancers and MIBC-specific enhancers, respectively.

3.5.3.8. Analysis of NMIBC and MIBC Microarray Data of patients

Expression data of the patients having bladder cancer (n=308) were obtained from GSE32894 Accession Code (62). The data was normalized by using Limma Bioconductor Package (63) “normalizeQuantiles” function. Patients’ samples were classified according to tumour stage by defining the ones with stage <T2 as NMIBC patients and >T2 as MIBC patients. Ggplot2 library’s “ggplot” function was used to obtain gene expression plots and “ggsignif” package was used to obtain significancy scores (Student’s t test).

3.5.3.9. Overlapping FRA1-FLI1 Peaks with MIBC-Specific Enhancers

Identified FRA1 and FLI1 peaks were separately overlapped with MIBC specific enhancers using “findOverlaps” function with “-type within” parameter in GenomicRanges library (56). Overlap rates were plotted using ggplot2 library (64).

3.5.3.10. Visualization of ChIP-Seq Reads

H3K27ac data which are aligned to GRHg38 were RPKM normalized with the help of deepTools Algorithm's "bamCovarage" command using the parameter "normalizeUsing RPKM" (65). Normalized reads were visualized using GViz R Bioconductor package in "horizon" type with "horizon.scale 50" parameters in "plotTracks" function (66). GeneRegionTrack was defined as GENCODE hg38 Comprehensive Gene Annotation Version 30 representing the annotation of the genes throughout genome (50).

3.5.3.11. Predicting the Target Genes of FRA1 and FLI1 on MIBC Specific Enhancer Regions

NMIBC and MIBC group specific enhancers regulating the target genes were overlapped with FRA1 and FLI1 peak regions using GenomicRanges package's "findOverlaps" function (56). Gene targets regulated by MIBC specific enhancers occupied by FLI1 or FRA1 or both were visualized using Gephi Software (version 0.9.2) (67).

3.5.3.12. Mass Spectrometry Data Analysis

Mass spectrometry and its analysis was performed in Francis Crick Institute with the help of Mahmoud-Reza Rafiee. Raw data obtained from Mass Spectrometry were analyzed using MaxQuant (1.6.2.6) with default settings (68). MSMS spectra were searched against the Uniprot databases (Human Swissprot) combined with a database containing protein sequences of contaminants. Enzyme specificity was set to trypsin/P and LysC, allowing a maximum of two missed cleavages. Cysteine carbamidomethylation was set as fixed modification, and methionine oxidation and protein N-terminal acetylation were used as variable modifications. Global false discovery rate for both protein and peptides were set to 1%. The match-between-runs and re-quantify options were enabled. Intensity-based quantification options (iBAQ) was also calculated.

Identified interactor proteins of FRA1 and FLI1 were filtered (adjusted p value < 0.05) and overlapped with top 100 co-dependent genes of *MAP4K4* and *FLOT1* genes by using the data provided by DepMap (69).

3.6. Plan and Schedule of The Research

Plan and Schedule of the research are represented below in Table 9.

Table 9. Plan and schedule of the research.

Time schedule	2018 December-2019 June	2019 March-2020 January	2019 November-2020 July	2020 March-2020 November	2020 February-2020 September	2020 September-2021 July	November 2020 - July 2021
Obtaining cell lines Maintaining the cell culture							
H3K27ac ChIP Library Preparation							
Sequencing of the ChIP samples Alignment of the data							
Finding MIBC and NMIBC Specific Enhancers and Bound Transcription Factors							
ChIP-SICAP experiments							
Knockdown RT-qPCR experiments							
FRA1 and FLI1 ChIP-Seq							

3.7. Evaluation of The Data

Significance score of the changes in mRNA expression is calculated by using unpaired, parametric t test.

3.8. Ethics Committee Approval

This thesis' proposal was given on July 2019. So, there is no need to ethics committee approval due to working with commercial human bladder cancer cell lines.

3.9. Restrictions of The Research

There are no restrictions of the research.

4. RESULTS

4.1. MIBC and NMIBC Specific Enhancers

Generated H3K27ac ChIP-Seq data is used to identify active regulatory regions in MIBC and NMIBC. 31911 number of active regulatory regions were identified for NMIBC (n=2) and 58206 number of H3K27ac peaks were found for MIBC group (n=4). 37% of NMIBC group's identified active regulatory regions overlapped with MIBC group's active regulatory regions (Figure 4a). The correlation of the read counts on active regulatory regions among cell lines is represented in Figure 4b which shows that cell lines were separated into groups by active regulatory regions. Differential active regulatory regions of two groups were then identified effectively as it can be seen from Figure 4c. Number of significantly (adjusted p value =< 0.05) differentially regulated enhancer regions of NMIBC is 295 while this number is 1404 for MIBC group. Two example snapshots representing one example region of NMIBC specific enhancers and one example region of MIBC specific enhancers are presented in Figure 4d-e, respectively.

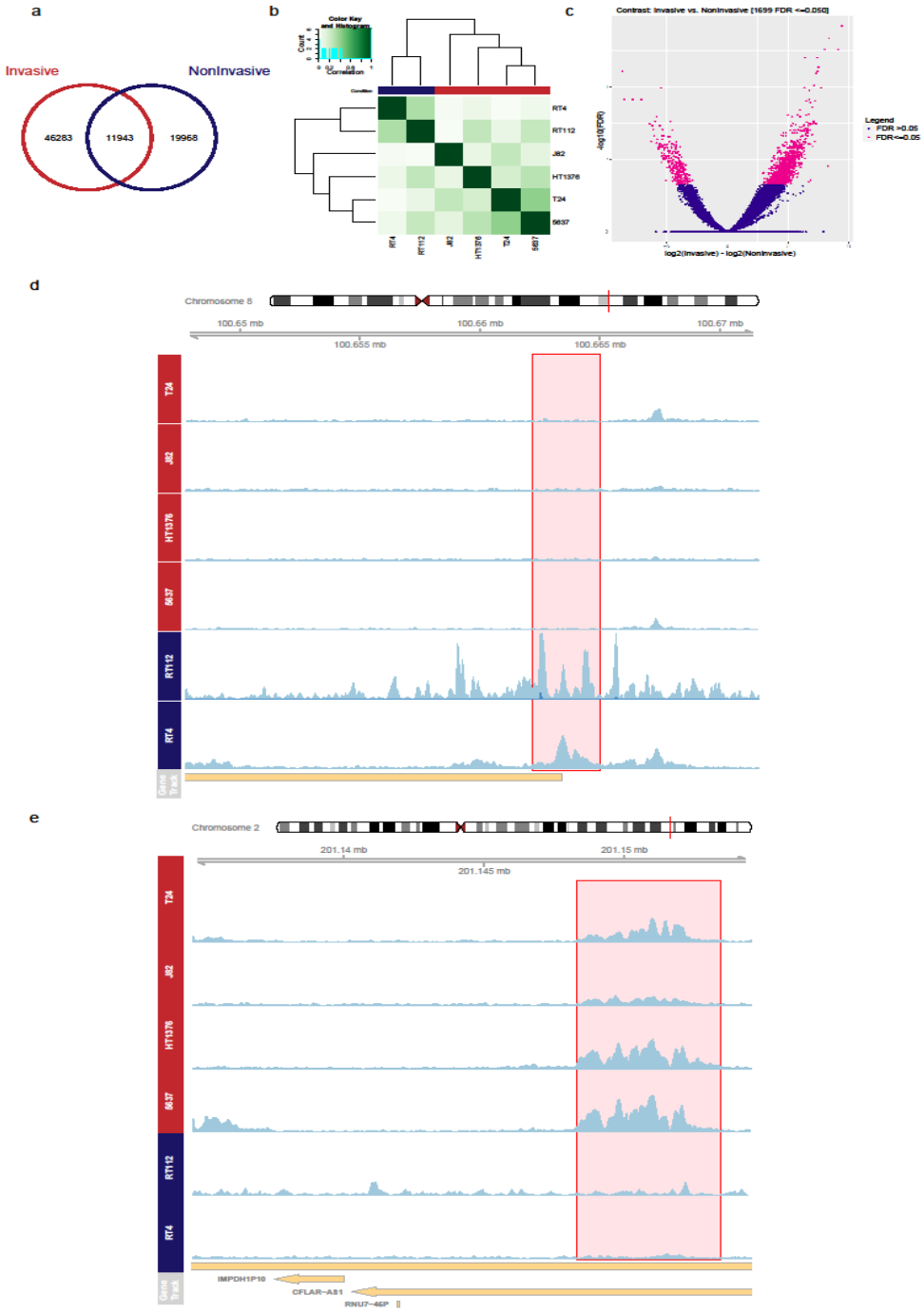

Figure 4. Active regulatory regions of NMIBC and MIBC. a. Representing the overlap of NMIBC and MIBC active regulatory regions. b. Heatmap representing correlation between the active regulatory regions of the cell lines. c. Volcano plot representing significantly differentially regulated active regulatory regions

of NMIBC and MIBC group. d. GViz figure representing an NMIBC specific enhancer region. e. GViz figure representing a MIBC specific enhancer region.

4.2. The Target Genes of NMIBC and MIBC Specific Enhancers

One step after defining NMIBC and MIBC specific enhancer regions, identifying the genes regulated by these regions was the next step. To find the target genes, GeneHancer database was used. Nearly 70% of the group specific enhancers were targeting one or more genes. In this step, it is important to consider the expression status of the target genes. Using Gaussian Mixture Modelling for clustering, all protein coding genes' RPKM values of bladder cancer cell line groups used in study were grouped as "expressed" and "not-expressed". Distribution of the gene expression values in NMIBC and MIBC groups were represented in Figure 5a-b. Genes having expression value more than -0.77 (log2 RPKM) were defined as "expressed" in NMIBC group while this cut-off is 0.98 (log2 RPKM) in MIBC group.

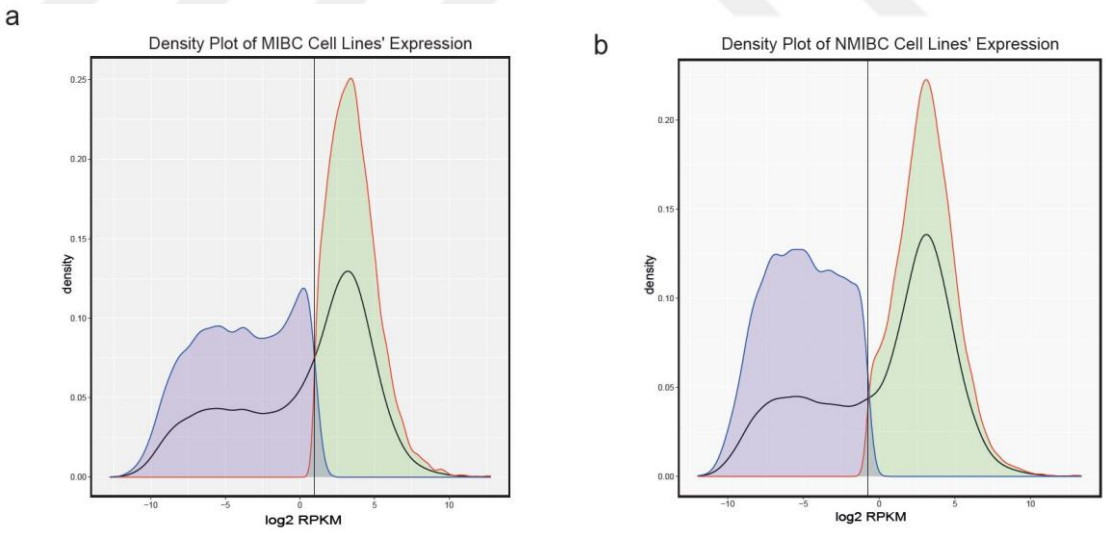

Figure 5. Density plot representing the density distribution of protein coding genes' expression values of different groups. a. Density plot of MIBC cell lines' expression log2 RPKM values. b. Density plot of NMIBC cell lines' expression log2 RPKM values.

Group specific enhancers mostly regulate single gene however there are also enhancers regulating more than one gene as it can be seen from the barplot in Figure 6a-b.

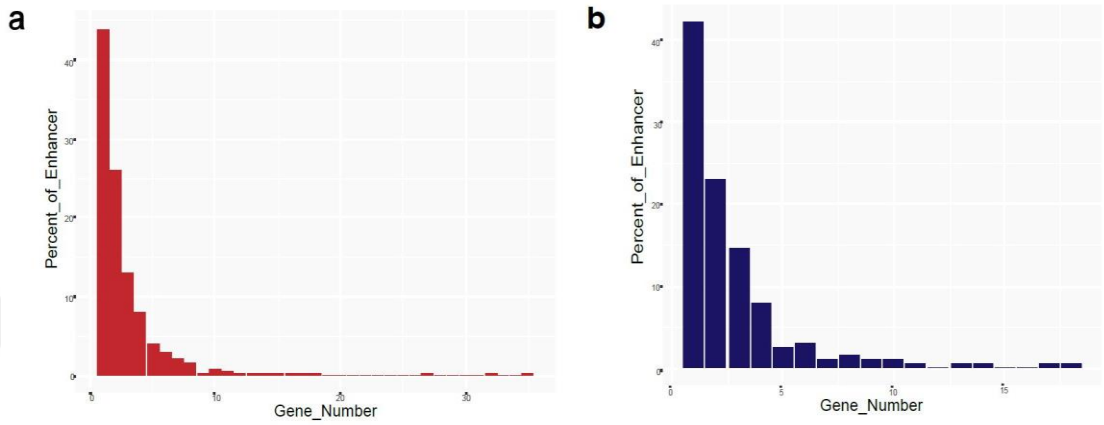

Figure 6. Representations of the number of enhancers regulating a gene or more than one genes among different groups. a. Barplot representing percent of MIBC enhancers and the number of genes regulated by. b. Barplot representing percent of NMIBC enhancers and the numbers of genes regulated by.

GO Term analysis of the target genes of NMIBC and MIBC specific enhancers show that most of the target genes of NMIBC group are implicated in regulation of transcription by RNA polymerase II (p adjusted value = 1.55e-05) while the target genes of MIBC group are involved in positive regulation of epithelial cell migration (p adjusted value = 9.21e-05), epithelium migration (p adjusted value =0.0004) and epithelial cell proliferation (p adjusted value = 0.00046) (Figure 7a-b).

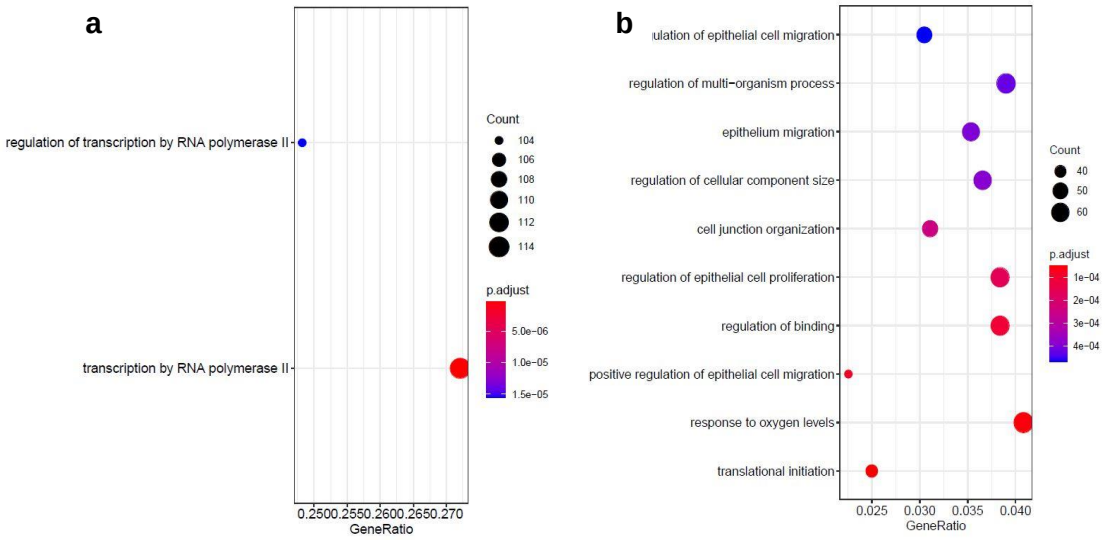

Figure 7. GO Terms enriched in different groups. a. Enriched Gene Ontology terms of NMIBC target genes. b. Enriched Gene Ontology terms of MIBC target genes.

Most of the NMIBC target genes are transcription factors (16.45%) which were defined by (70). However in MIBC target genes, there are *TGFB2*, *CDH2*, *HIF1A* genes regulating epithelial to mesenchymal transition (71-73). These results imply that target genes of NMIBC target genes are transcription factors which might be important for maintenance of proper urothelium structure while MIBC target genes are involved in epithelial cell migration thus probably having a crucial role in the invasion to muscle. Example snapshots visualizing MIBC specific enhancer regulating *TGFB2* and NMIBC specific enhancer regulating *FGFR3* are represented in Figure 8a-b, respectively.

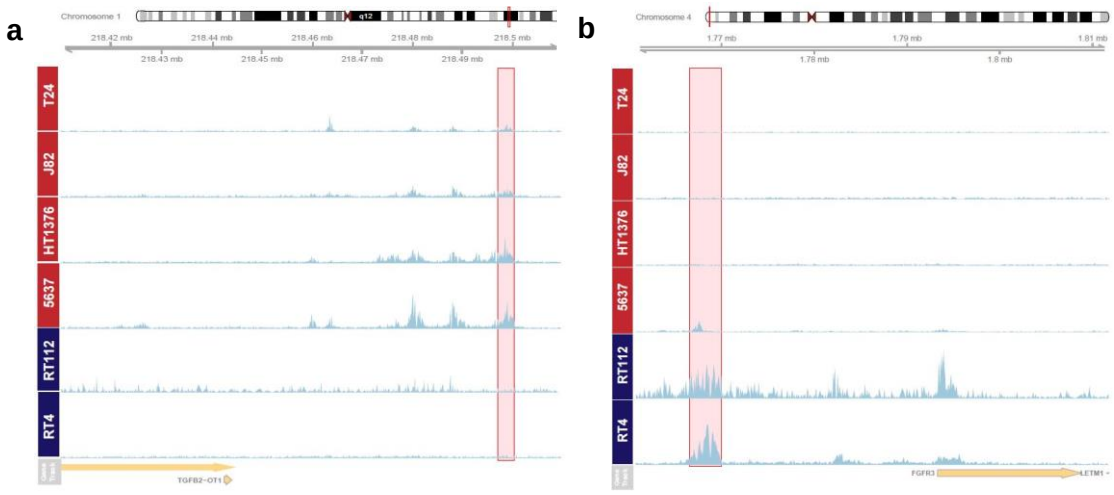

Figure 8. Examples of MIBC and NMIBC specific enhancers. a. MIBC specific enhancer region (highlighted with red) regulating TGFB2 gene expression. b. NMIBC specific enhancer region (highlighted with red) regulating FGFR3 gene expression.

4.3. Transcription Factors Motifs on NMIBC and MIBC Specific Enhancers

Motif search on NMIBC and MIBC specific enhancers unearthed the transcription factors that can bind to the nucleosome free regions of the enhancers. *ATF3*, *FRA1*, *JUNB* and *AP-1* transcription factors are at the top of the transcription factor motif list of MIBC specific enhancers as can be seen in Figure 9. *Tp63*, *Tp73*, *Tp53* and *PPARɣ* motifs are at the top of motif finding analysis on NMIBC specific enhancers when the significance scores are considered as it can be seen from Figure 10.

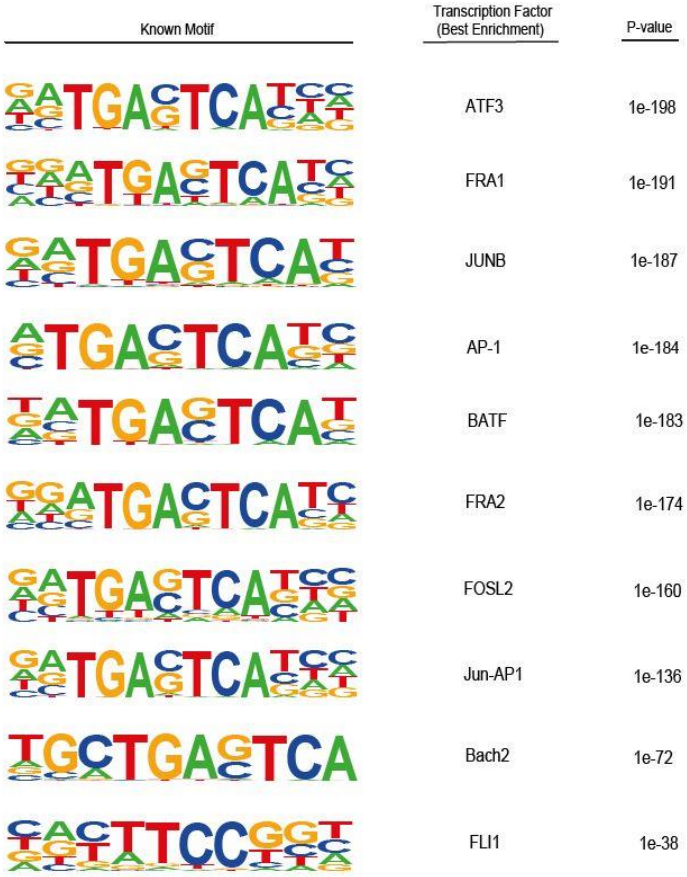

Figure 9. Top 10 transcription factor motifs enriched on MIBC specific enhancers.

Figure 10. Top 10 transcription factor motifs enriched on NMIBC specific enhancers.

Finding out enriched transcription factor motifs is not enough to interpret which transcription factors are playing role in building NMIBC and MIBC characteristics. Thus, differential expression status of the top 10 transcription factors enriched for NMIBC and MIBC groups was checked. In this regard, *FRA1* is the best transcription factor candidate whose expression is significantly higher in MIBC group than NMIBC according to both cell line (CCLE (60)) (p value = 0.043) (Figure 9b) and primary bladder cancer tissue gene expression data (p value = 0.0066) (Figure 10a). Besides, *FLI1* is the second transcription factor among the rest of the transcription factors that have the highest significance score in terms of being overexpressed in MIBC (p value for cell line groups = 0.1, p value for tissue groups = 0.07). Boxplot representing the

differential expression of *FLI1* in cell line groups is shown in Figure 11b and Figure 12a represents the differential expression in tissue groups. On the other hand, *Tp63* is significantly higher expressed in NMIBC cell line group (p value = 0.046) (Figure 11d) and also in NMIBC primary tissue samples (p value = 6.3e-06) (Figure 12b). *GRHL2* is the other one significantly higher expressed gene in NMIBC tissue group (p value = 0.015) as it can be seen from Figure 12b yet it is not significantly overexpressed in NMIBC cell line group (p value = 0.09) as it is shown in Figure 11d. *PPARɣ* is another crucial transcription factor that has significantly higher expression in NMIBC groups both in cell line (p value = 0.049) (Figure 11b) and primary tissue (p value = 3.2e-10) (Figure 12b).

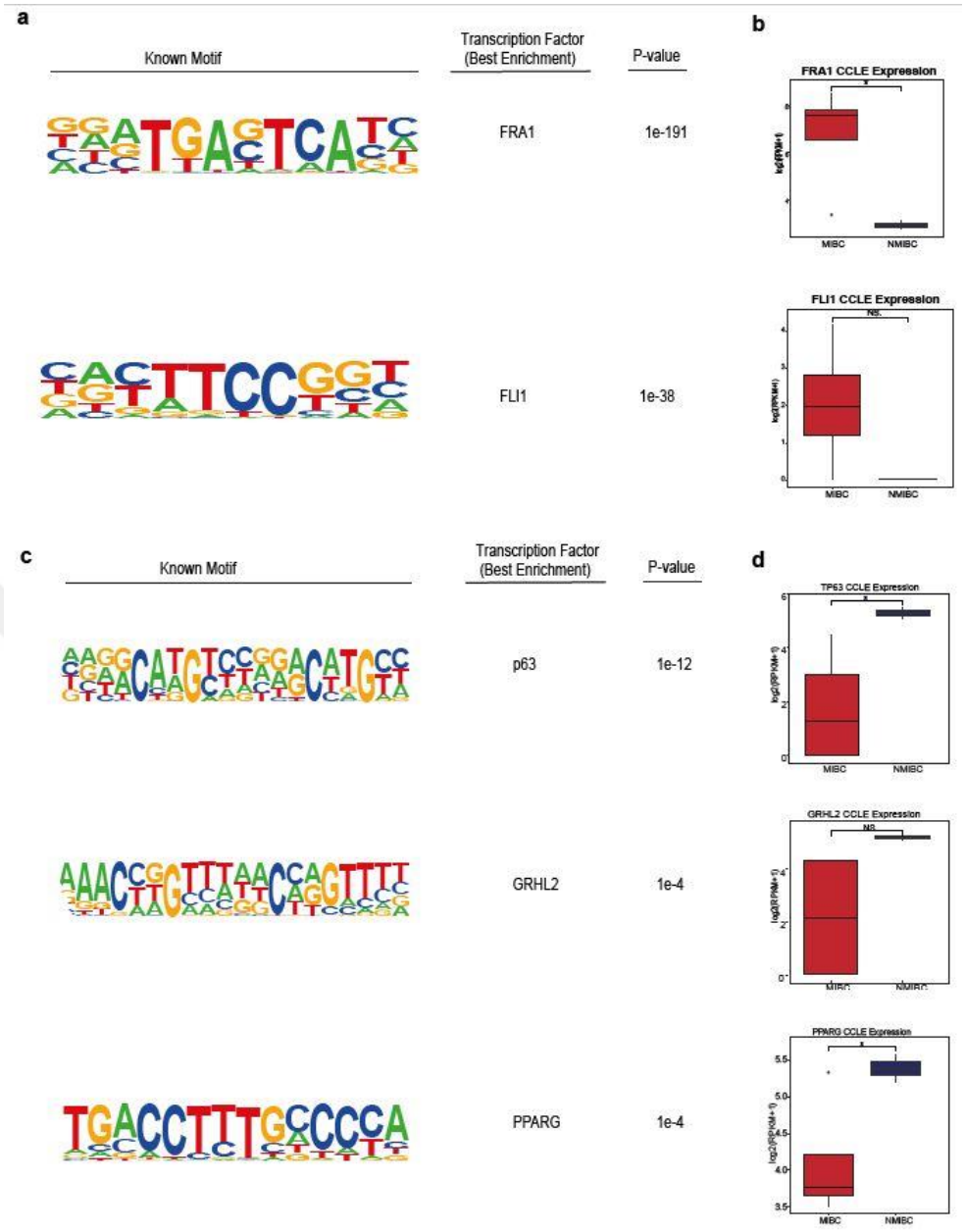

Figure 11. Transcription factor motifs and their expression values among MIBC and NMIBC group. a. Transcription factor motifs that are crucial in MIBC characterization. b. Boxplots representing the expression difference between MIBC and NMIBC cell line groups. c. Motifs of transcription factors that are differentially expressed in NMIBC cell line group. d. Boxplots showing the difference of expression in cell line groups.

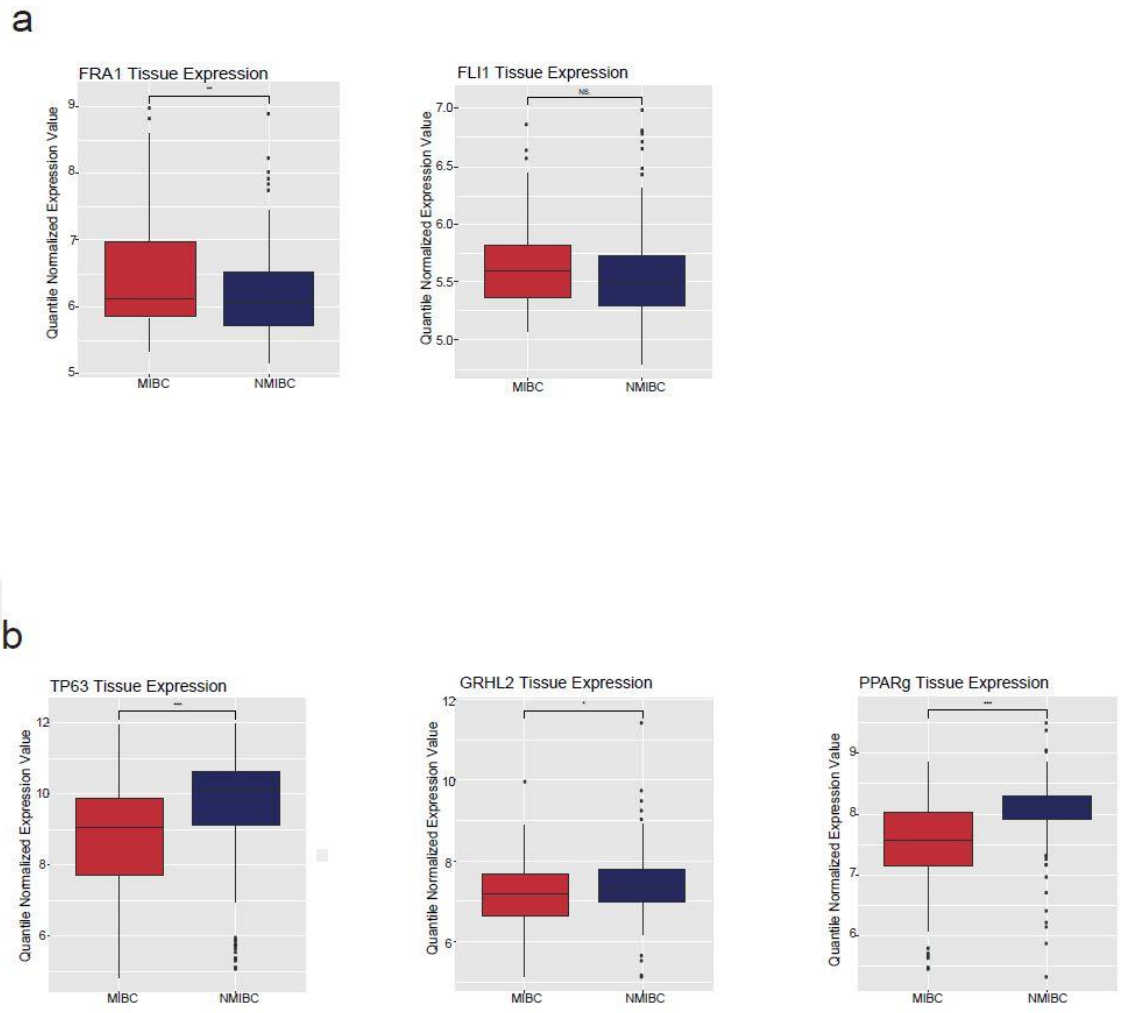

Figure 12. Differential expression of candidate transcription factors among MIBC and NMIBC tissue samples. a. Tissue expressions' difference between NMIBC and MIBC of FRA1 and FLI1. b. Tissue expressions' difference between NMIBC and MIBC of Tp63, GRHL2 and PPARɣ.

4.4. Gene Targets of FRA1 and FLI1 Bound MIBC Specific Enhancers

3834 peaks are identified as FLI1 peak regions while 31918 peaks are identified as FRA1 peak regions. FRA1 and FLI1 peak regions overlapped with MIBC specific enhancers with the rates 7.8% and 65.3%, respectively. However overlap of the NMIBC specific enhancers with FLI1 and FRA1 peaks are low, 0% and 1.6%, respectively. The rates of the overlapping peak regions were represented in Figure 13.

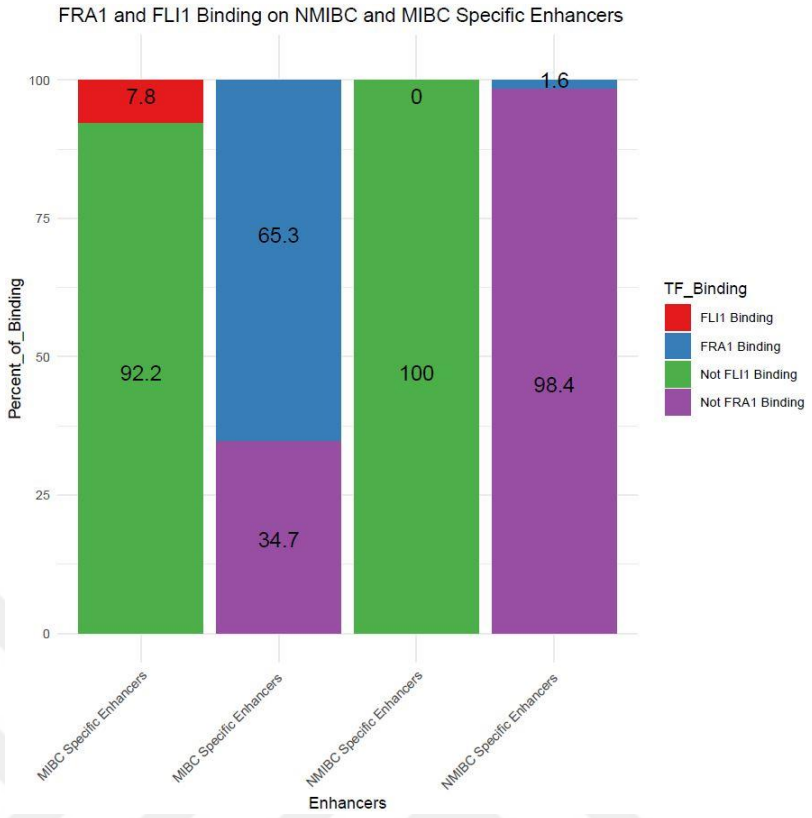

Figure 13. Overlap of FRA1 and FLI1 peaks with NMIBC and MIBC specific enhancers.

Among gene targets of all MIBC specific enhancers (1752 genes), 854 genes are identified as possible gene targets of FRA1 while 201 genes are possible gene targets of FLI1 on MIBC specific enhancers. 200 numbers of FLI1 target genes are also FRA1 target genes as can be seen from Figure 14.

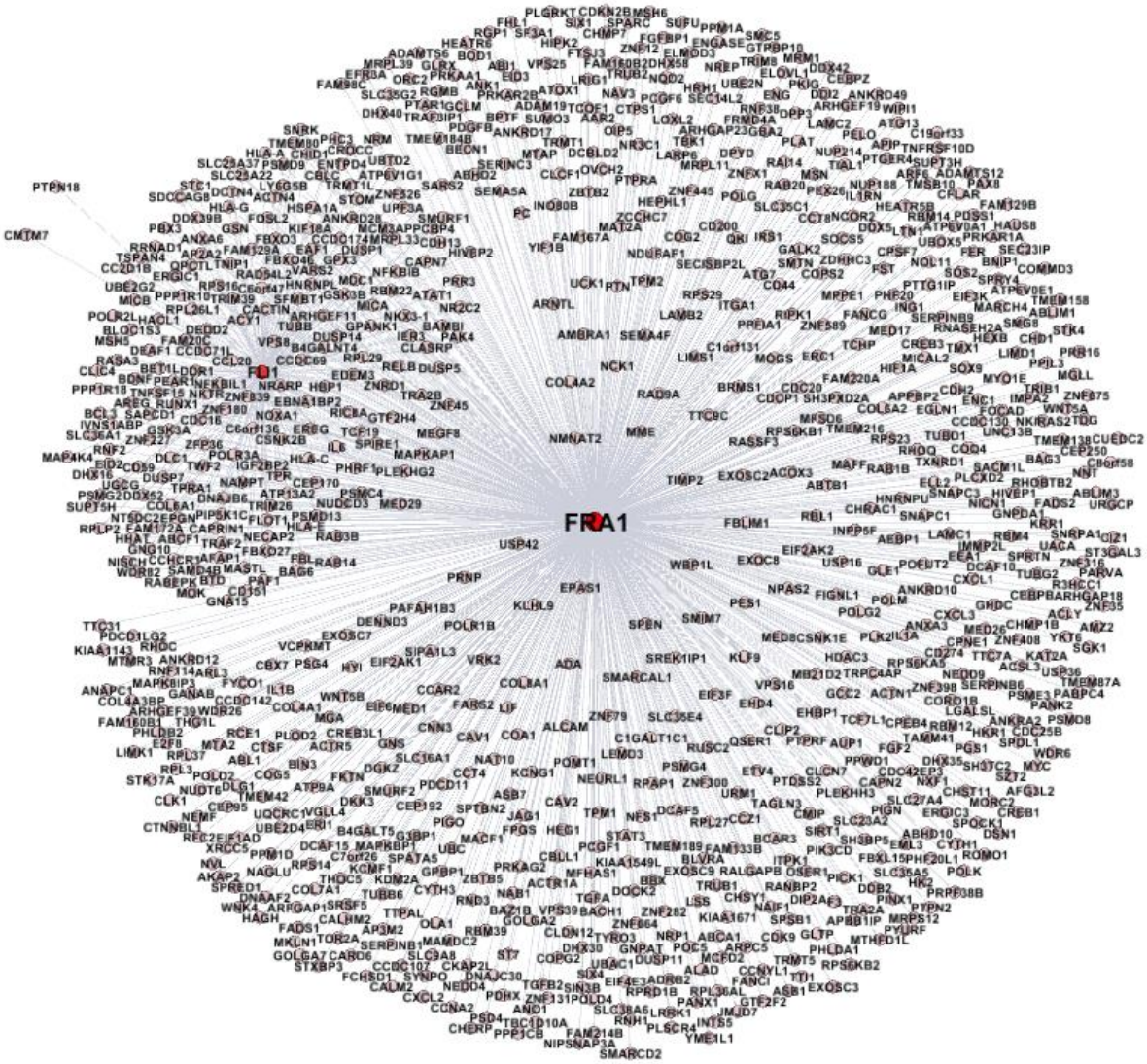

Figure 14. Identified FLI1 and FRA1 transcription factors' target genes.

Identified FLI1 and FRA1 gene targets filtered by selecting the genes implicated in GO Terms shown in Figure 7b including the keywords "migration" and "cell junction organization". A representative figure including the filtered target genes and its regulatory protein is shown in Figure 15.

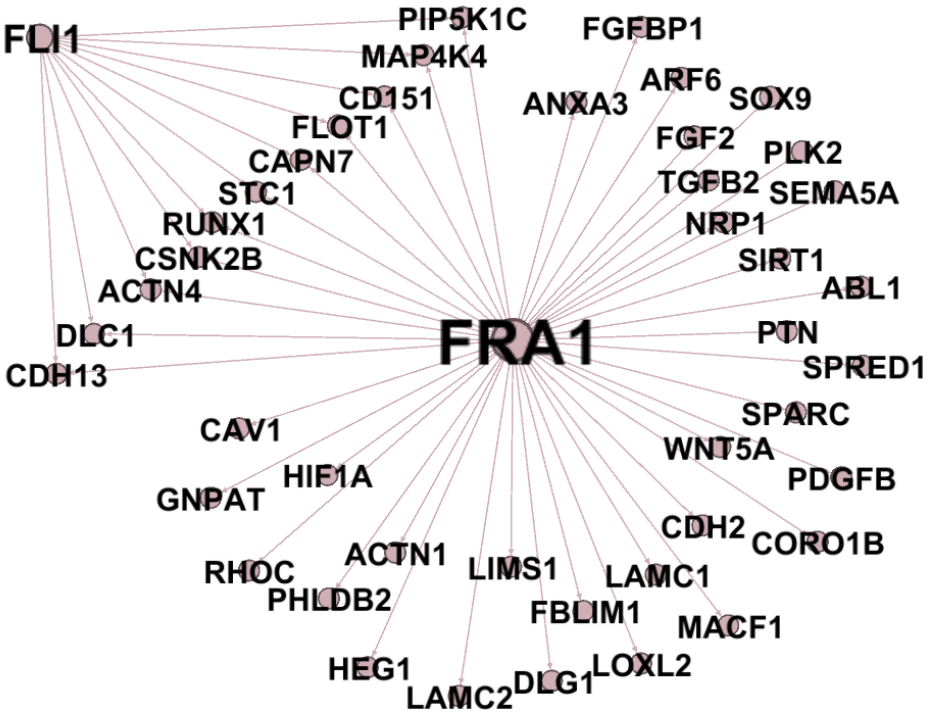

Figure 15. FRA1 and FLI1 target genes implicated in “positive regulation of epithelial cell migration”, “epithelium migration”, “regulation of epithelial cell migration” or “cell junction organization” GO Terms.

4.5. FRA1 and FLI1 Knockdown Leads to Downregulation In MAP4K4 and FLOT1 Genes Implicated In Epithelial Cell Migration and Cell Junction Organization

Unique FRA1 and FLI1 siRNA knockdowns resulted in nearly 60% decrease in both protein and mRNA levels of *FRA1* and *FLI1,* respectively. Graphs representing the changes in mRNA and protein level and western membranes showing the changes in protein levels are can be seen from Figure 16a and Figure 16b. On the other hand, double knockdown (FLI1 + FRA1 together) did not yield a significant change in protein levels, as shown in Figure 16a-b.

MAP4K4 gene is one of the target genes of both FLI1 and FRA1 as it can be seen from Figure 15. Both FRA1 an FLI1 unique knockdown resulted in nearly 50% decrease in *MAP4K4* gene mRNA levels (Figure 16c). *FLOT1* is another co-target gene of FLI1 and FRA1 and its expression level was

decreased up to 50% after FLI1 knockdown and nearly 30% after FRA1 knockdown. Graph showing changes in mRNA levels of *FLOT1* can be seen from Figure 16c.

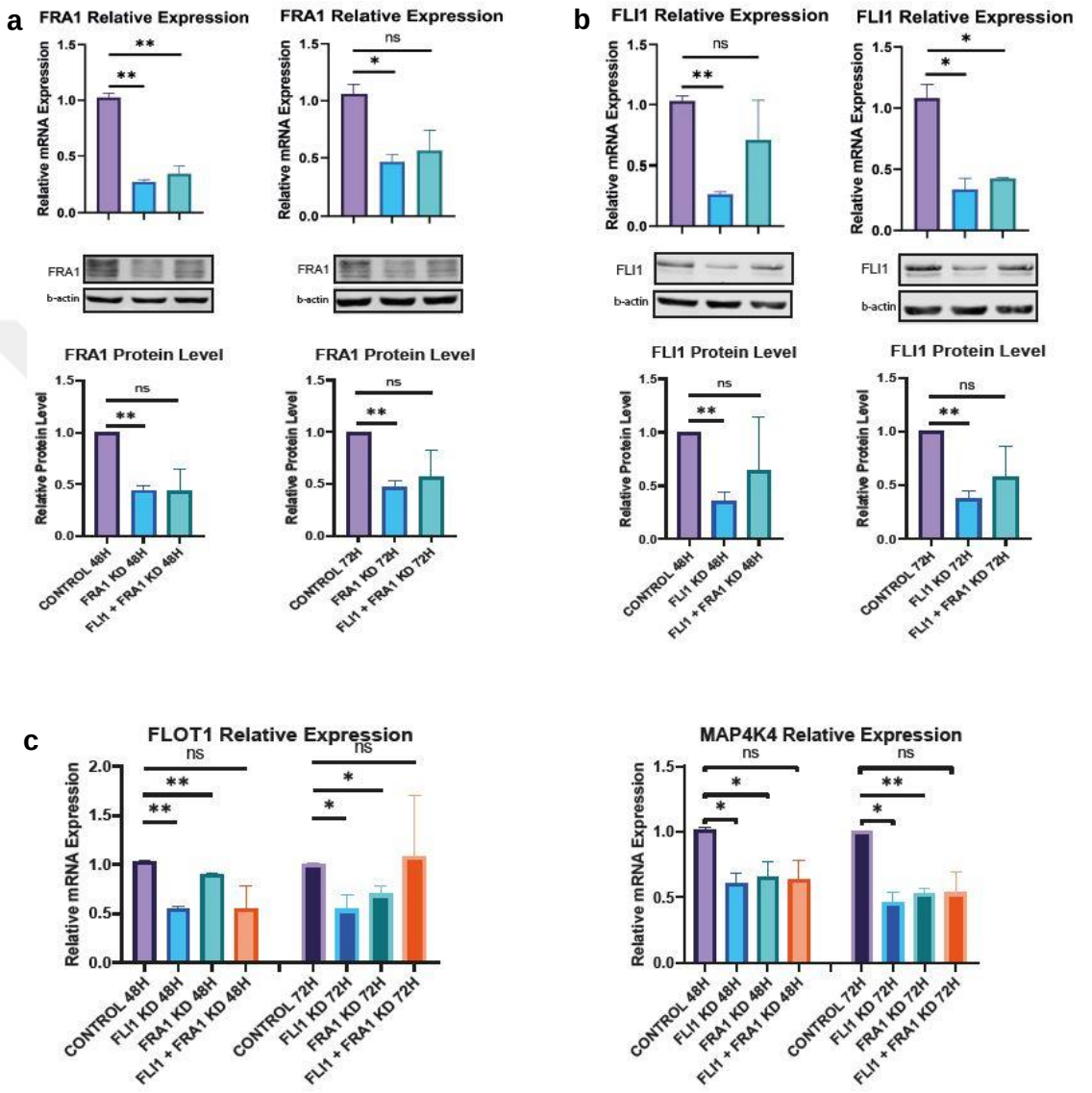

Figure 16. Changes in protein and mRNA levels after knockdown experiments. a. Changes in FRA1 mRNA and protein levels after 48 hours and 72 hours from knockdown.b. Changes in FLI1 mRNA and protein levels after 48 hours and 72 hours from knockdown. c. Changes in FLOT1 and MAP4K4 mRNA levels after 48 hours and 72 hours from knockdown. (n=2 biological replicates, error bars are representing -/+SD of the mean, unpaired and parametric t-test was used, * p value < 0.05, ** p value < 0.005, ns means the change is not significant).

4.6. SWI/SNF Complex Is Implicated In Gene Regulation via Interacting with FRA1 and FLI1

ChIP-SICAP experiments identified 1436 numbers of co-regulatory proteins of *FRA1* and 103 numbers of co-regulatory proteins of *FLI1* transcription factor (log FC >1, adjusted p value < 0.1). Most of the proteins identified are located in the nucleus and chromosome as it can be seen from Figure 15a indicating the efficiency of ChIP-SICAP experiment. Scatter plots showing the correlation between ChIP-SICAP replicates for both FRA1 and FLI1 (Figure 17b-c) highlight some critical chromatin proteins implicated in gene regulation. Both FRA1 and FLI1 are also identified in the interactomes of FRA1 and FLI1 ChIP-SICAP experiments, demonstrating the specifity.

Important components of SWI-SNF Complex (BAF) were identified as FRA1 interactors such as ACTL6A, ACTB, SMARCA4, SMARCE1, SMARCC1 and SMARCB1. On the other hand, SMARCC2 from this complex is one of the interactor of FLI1.

In this study, *MAP4K4* gene is reported as one of the genes regulated by FRA1 and FLI1 transcription factors. We integrated our ChIP-SICAP data with the data present in DepMap (69). Our results show that MAP4K4 co-dependent genes *IQGAP1*, *FHL2*, *PARP2* and *CAB39* proteins are identified as FRA1 interactors. *FLOT1* was the other gene which is determined to be regulated by FRA1 and FLI1 in this thesis. Integration of ChIP-SICAP and DepMap for *FLOT1* gene showed that *CLIC1*, *REXO4*, *GNL1* and *FAM50A* are interactor partners of FRA1 (69). However there is not any overlap with FLI1 interactors and FLOT1 co-dependent proteins. Based on all this results, hypothetical regulatory schemes for *MAP4K4* and *FLOT1* are constituted (Figure 18).

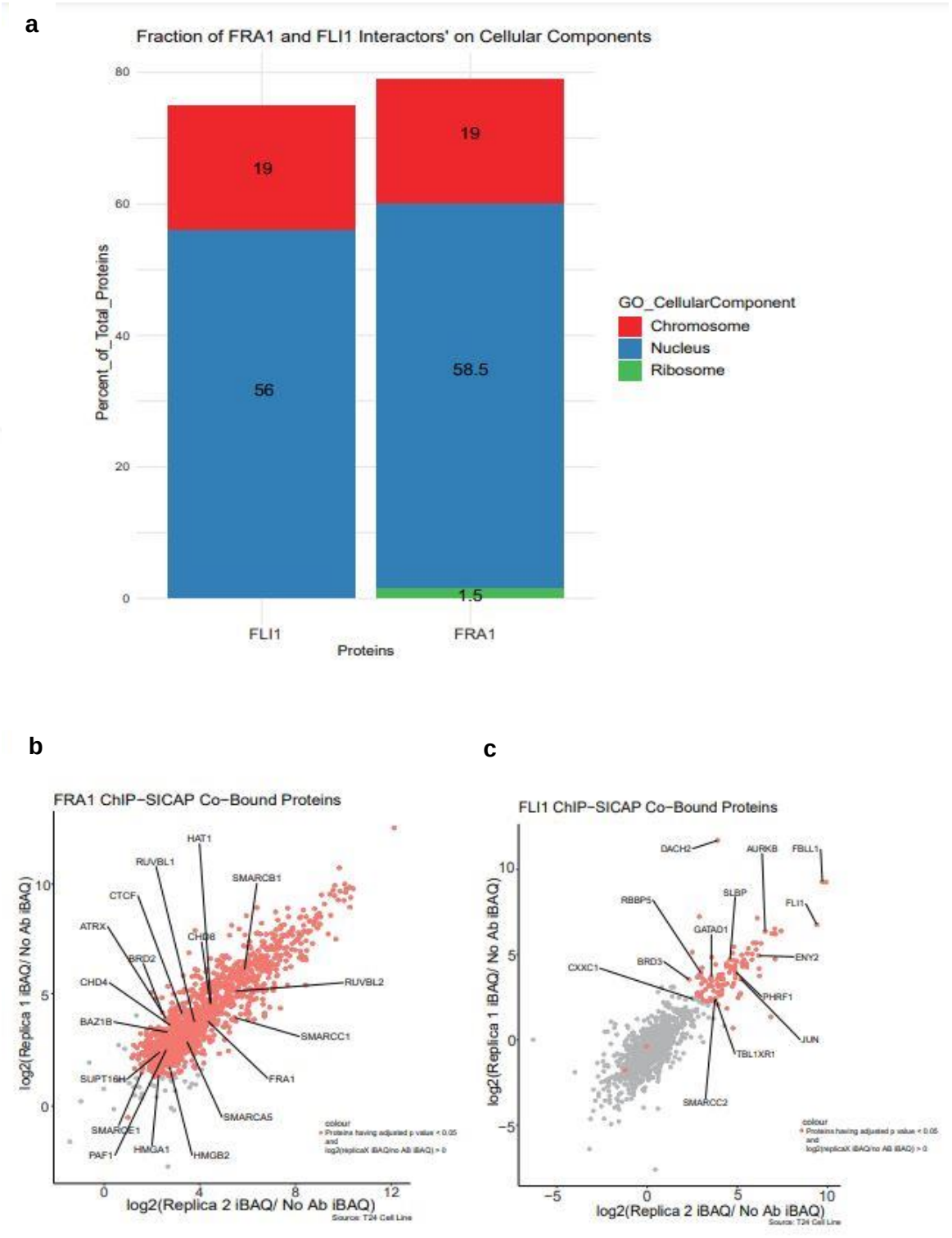

Figure 17. A general representation of FRA1 and FLI1 ChIP-SICAP experiment results. a. FRA1 and FLI1 interactor proteins' distribution in cellular components (proteins with fold change > 1 and adjusted p value < 0.1). b. Scatterplot of the

FRA1 (left) and FLI1 (right) ChIP-SICAP replicates. Values in x and y axis represent log2 iBAQ values of replicates normalized to no antibody control. Identified proteins with adjusted p value < 0.05 are shown in red color.

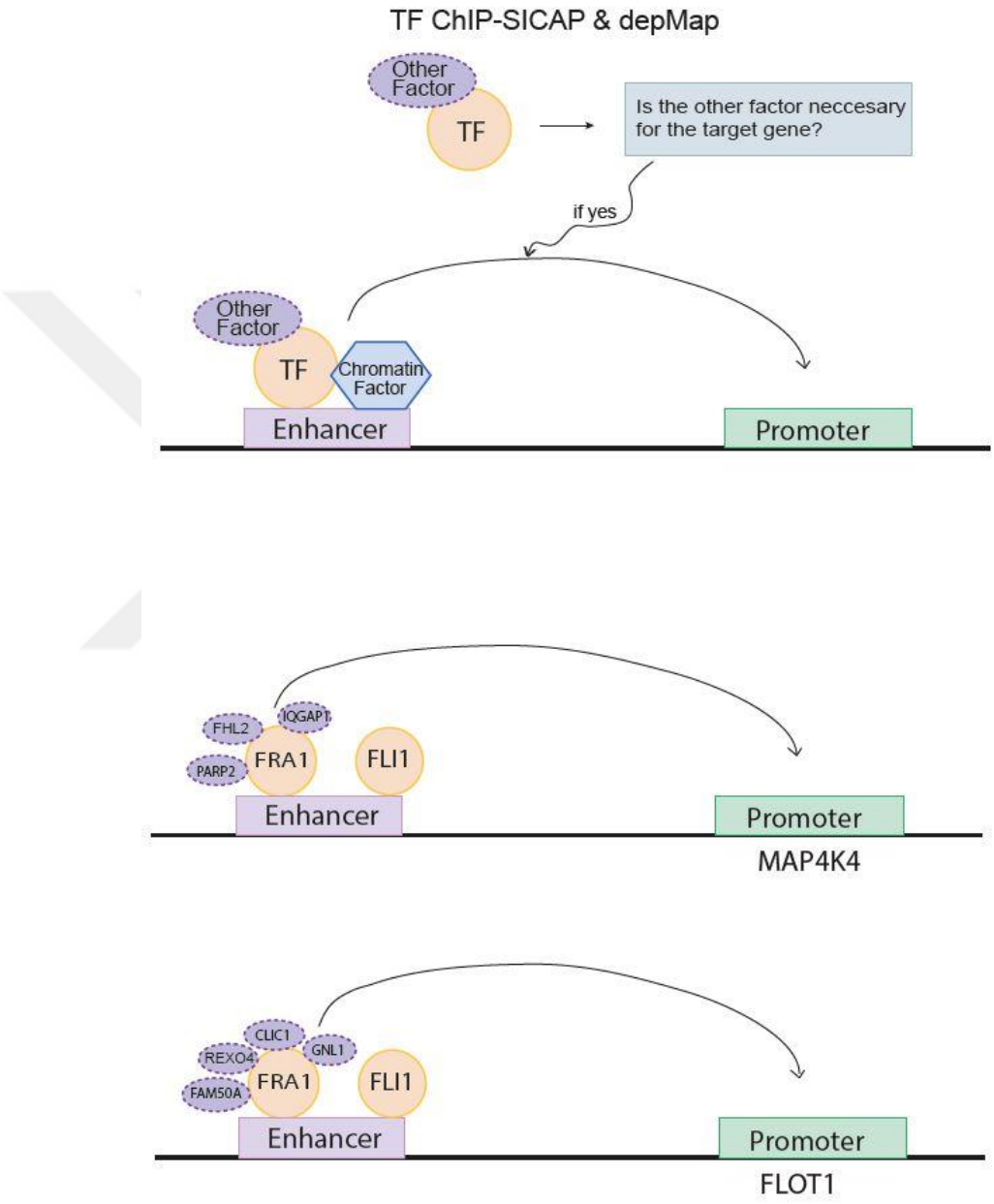

Figure 18. Hypothetical transcriptional regulation mechanisms of MAP4K4 and FLOT1 genes. Line dash means physical interaction may not occur with the nearest protein.

5. DISCUSSION

The aim of this thesis was characterizing MIBC and NMIBC groups according to gene regulatory mechanisms via identifying differential enhancers. Differential active regulatory regions of MIBC and NMIBC groups were identified and their target genes and transcription factors enriched at these enhancers were reported.

In NMIBC group, *GRHL2* transcription factor was one of the transcription factor found enriched at NMIBC specific enhancers. Its expression is significantly higher in NMIBC group in tissue samples. Recently, *GRHL2* is defined as “anti-oncogene” and preventing epithelial to mesenchymal transition in bladder cancer cell lines by regulating *ZEB1* (74). Its metastasis reducing effect is also shown in gastric cancer (75), colorectal cancer (76) and prostate cancer (77). Epithelial state of the cells were maintained with GRHL2-miR 200-ZEB1 co-operation in ovarian cancer (78). *Tp63* is another transcription factor determined to be enriched at NMIBC specific enhancers. Its role in driving the basal-like phenotype in urothelium is well defined, suppressing differentiation by triggering the expression of basal markers (79). In bladder cancer, Tp63 is reported to be in the opposite direction of gene expression with some Zeb family transcription factors in tumour samples yet, surprisingly, DNp63 isoform overexpression is positively correlated with low survival of the patients (80). Like *Tp63*, *PPARɣ* is another transcription factor enriched at NMIBC specific active regulatory regions which has also significantly higher expression levels in both tissue samples and cell lines. Although it has a role in pre-adipocyte to adipocyte transition (81), it has also a defined role as a tumour suppressor in bladder tumours in a pre-print (82). It is also reported that silencing *PPARɣ* results in decrease in invasion of bladder cancer cell lines by regulating AKT-GSK3β pathway (83). In another study performed with bladder cancer cell lines, *PPARɣ* is highlighted as a candidate therapeutic target of bladder cancer due to the decrease in proliferation of bladder cancer cell lines when *PPARɣ* is inactivated (84). Considering all of the knowledge together, it can be said that *GRHL2*, *Tp63* and *PPARɣ* transcription factors have crucial roles characterizing NMIBC however when the target genes of NMIBC specific enhancers is considered; most of the target genes were transcription factors which are most likely associated with preservation of epithelial characteristics but could not be

directly linked to NMIBC regulation. Because of this reason, thesis project was continued with exploring the gene regulatory mechanisms characterizing MIBC group.

In MIBC group, among top ten transcription motifs enriched at differential enhancers, *FRA1* transcription factor was the one significantly differentially expressed in MIBC group in both tissue samples and cell lines. FRA1 transcription factor was one of the Fos family members, previously identified to enhance cell motility of bladder cancer cell lines (35) and it was also reported to increase metastasis ability of breast cancer cell lines (85). Besides, in colorectal cancer, epithelial to mesenchymal transition is found to be dependent to *FRA1* expression (86). *FRA1*'s positive regulation of metastasis and proliferation is also reported in squamous cell carcinoma (87). In triple negative breast cancer, its down regulatory and up regulatory effects on genes were well defined, together with *FRA2* or uniquely (88). Another transcription factor enriched at MIBC specific active regulatory regions is *FLI1* which is over-expressed in MIBC cell lines (p value = 0.1) and tissue samples with borderline significance (p value = 0.07). *FLI1* transcription factor is mostly known with its role in development of erythroleukemia (89). On the other hand, *FLI1* is needed for hematopoietic stem cell development (90, 91), indirectly regulates the expression of *VE-statin/egfl7* which is expressed in endothelial cells (92) and it is one of the activator of *Endoglin* gene expressed during angiogenesis (93). Besides, overexpression of *FLI1* leads to a switch from epo-induced differentiation state to proliferative state in erythroblasts (91). In this thesis, *FLI1* transcription factor is defined as a regulator of muscle invasion in bladder cancer cell lines for the first time.

Identifying *FRA1* and *FLI1* transcription factors as activators of muscle invasion in bladder cancer was followed by defining their target genes and observing the molecular changes after they are silenced. Unique knockdown of *FRA1* and *FLI1* genes lead to a decrease in the expression of *MAP4K4* and *FLOT1* genes. This result shows that *FRA1* and *FLI1* genes activate the expression of *MAP4K4* and *FLOT1* genes via binding to MIBC specific enhancers located at chr2:101514957-101521268 while activating *MAP4K4* expression and chr6:30768451-30770663 and/or chr6:30780705-30783488 located enhancers to

induce *FLOT1* gene expression. *MAP4K4* gene is known to promote invasion in medulloblastoma cells (94), support metastasis in hepatocellular carcinoma when JNK and NF-kB pathways are activated (95), crucial for the invasion of glioblastoma (96). Moreover, in T24 cell line, downregulation of *MAP4K4* gene leads to a decrease in both proliferation ability of the cells and invasion (97). *FLOT1* gene is also reported as supporting proliferation and recurrence in bladder cancer tissue samples and its overexpression is related with invasion of the bladder cancer cells (98). *FLOT1* also induces epithelial to mesenchymal transition in lung adenocarcinoma by affecting ERK/Akt pathway (99). Another study reported that degradation of Snail protein in prostate cancer is prevented by sumoylated *FLOT1* gene indirectly leading epithelial to mesenchymal transition (100). Overall, in this thesis, *MAP4K4* and *FLOT1* genes are found to be regulated by FRA1 and FLI1 transcription factors and characterizing MIBC.

In this thesis, co-partner proteins of FRA1 and FLI1 transcription factors are tried to be found using ChIP-SICAP method. SWI-SNF Complex (BAF) proteins ACTL6A, ACTB, SMARCA4, SMARCE1, SMARCC1 and SMARCB1 are identified as co-partner of FRA1 indicating cooperation between SWI/SNF Complex and FRA1 in transcriptional regulation. BAF Remodelling Complex is ATP dependent and has ability to change chromatin dynamics thus regulating gene expression and it is crucial for neural development (101). BAF Complex's activity is also reported as essential for embryonic development and loss of its subunits results in H3K27me3 accumulation and deregulates embryogenesis and forebrain development (102). In this manner, identifying many of the subunits in BAF complex as FRA1 co-partner proteins indicates that BAF Complex components regulate the opening of chromatin at MIBC enhancers. On the other hand, there was just one protein from BAF Complex in FLI1 interacting proteins but this can be because of the different efficiencies of FRA1 and FLI1 ChIP-SICAP experiments as well; when it is considered that less number of FLI1 interacting proteins was identified compared to FRA1.

Other proteins implicated in transcriptional machinery characterizing MIBC group are predicted by using Cancer Dependency Map (DepMap) (69). Considering dependency between experimentally validated gene targets (*MAP4K4* and *FLOT1*)

and FRA1 or FLI1 interactors, co-partner proteins of FRA1 and FLI1 that have a role in the regulation of *MAP4K4* and *FLOT1* genes are predicted. Among the genes *MAP4K4* to be dependent on, *IQGAP1*, *FHL2*, *PARP2* and *CAB39* overlapped with the FRA1 SICAP interactors. IQGAP1 is a protein that functions in both nucleus and cytoplasm and having distinct roles and far-going interactors (103). FHL2 is a transcriptional regulatory protein known to be regulating the expression of *p21* with the guidance of matrix mechanics (104). PARP2 protein has crucial role in DNA repair (105) and overexpressed in acute myeloid leukemia patients (106). CAB39 is another FRA1 interactor protein however its function in nucleus is not defined and known as a cytosolic protein so it is not thought to be in transcriptional regulation of *MAP4K4*. On the other hand, there are not any overlapping FLI1 interactors among the genes *MAP4K4* is dependent probably because of the low efficiency of FLI1 SICAP experiment.

FLOT1 is the other target gene of FRA1 and FLI1 at MIBC specific enhancers. Genes dependent on according data in DepMap overlapped with CLIC1, REXO4, GNL1 and FAM50A FRA1 SICAP interactor proteins. CLIC1 can be found both in nucleus, cytoplasm and the membrane of the cells and reported as enhancing cancer cells invasion ability (107), supporting progression of gastric cancer via MAPK/AKT pathways (108). REXO4 protein is one of the DNA binding proteins yet its biological function is not defined yet. GNL1 protein is a nucleolar GTPase and reported as overexpressed in bladder cancer (109). FAM50A is a nuclear localization signal carrying potential transcription factor which is reported to support ameloblast differentiation by physically interacting with RUNX2 (110).

6. CONCLUSION AND FUTURE ASPECTS

FRA1 and FLI1 transcription factors are possible drivers of invasion to muscle in bladder cancer cell lines by regulating MAP4K4 and FLOT1 genes' expression. Transcriptional regulatory complex of FRA1 potentially includes IQGAP1, FHL2 and PARP2 proteins while regulating MAP4K4 gene expression while CLIC1, REXO4, GNL1 and FAM50A proteins might be in complex with FRA1 for regulation of FLOT1 expression. Most of the component proteins of BAF Complex of SWI/SNF Complex are found as FRA1 interactors indicating highly dynamic chromatin

structure. In this manner, targeting MAP4K4 or FLOT1 can be good targets in the treatment of MIBC.

7. REFERENCES

1. Waddington CH. The epigenotype. 1942. Int J Epidemiol. 2012;41(1):10-3.
2. Wu C, Morris JR. Genes, genetics, and epigenetics: a correspondence. Science. 2001;293(5532):1103-5.
3. Verhoeven KJ, vonHoldt BM, Sork VL. Epigenetics in ecology and evolution: what we know and what we need to know. Mol Ecol. 2016;25(8):1631-8.
4. Dupont C, Armant DR, Brenner CA. Epigenetics: definition, mechanisms and clinical perspective. Semin Reprod Med. 2009;27(5):351-7.
5. Kagohara LT, Stein-O'Brien GL, Kelley D, Flam E, Wick HC, Danilova LV, et al. Epigenetic regulation of gene expression in cancer: techniques, resources and analysis. Brief Funct Genomics. 2018;17(1):49-63.
6. Hanahan D, Weinberg RA. Hallmarks of cancer: the next generation. Cell. 2011;144(5):646-74.
7. Flavahan WA, Gaskell E, Bernstein BE. Epigenetic plasticity and the hallmarks of cancer. Science. 2017;357(6348).
8. Darwiche N. Epigenetic mechanisms and the hallmarks of cancer: an intimate affair. Am J Cancer Res. 2020;10(7):1954-78.
9. Allis CD, Jenuwein T. The molecular hallmarks of epigenetic control. Nat Rev Genet. 2016;17(8):487-500.
10. Tie F, Banerjee R, Stratton CA, Prasad-Sinha J, Stepanik V, Zlobin A, et al. CBP-mediated acetylation of histone H3 lysine 27 antagonizes Drosophila Polycomb silencing. Development. 2009;136(18):3131-41.
11. Schoenfelder S, Fraser P. Long-range enhancer-promoter contacts in gene expression control. Nat Rev Genet. 2019;20(8):437-55.
12. Creyghton MP, Cheng AW, Welstead GG, Kooistra T, Carey BW, Steine EJ, et al. Histone H3K27ac separates active from poised enhancers and predicts developmental state. Proc Natl Acad Sci U S A. 2010;107(50):21931-6.
13. Johnson DS, Mortazavi A, Myers RM, Wold B. Genome-wide mapping of in vivo protein-DNA interactions. Science. 2007;316(5830):1497-502.

14. Furey TS. ChIP-seq and beyond: new and improved methodologies to detect and characterize protein-DNA interactions. Nat Rev Genet. 2012;13(12):840-52.
15. Rafiee MR, Girardot C, Sigismondo G, Krijgsveld J. Expanding the Circuitry of Pluripotency by Selective Isolation of Chromatin-Associated Proteins. Mol Cell. 2016;64(3):624-35.
16. Sung H, Ferlay J, Siegel RL, Laversanne M, Soerjomataram I, Jemal A, et al. Global Cancer Statistics 2020: GLOBOCAN Estimates of Incidence and Mortality Worldwide for 36 Cancers in 185 Countries. CA Cancer J Clin. 2021;71(3):209-49.
17. Sanli O, Dobruch J, Knowles MA, Burger M, Alemozaffar M, Nielsen ME, et al. Bladder cancer. Nat Rev Dis Primers. 2017;3:17022.
18. Kamoun A, de Reynies A, Allory Y, Sjodahl G, Robertson AG, Seiler R, et al. A Consensus Molecular Classification of Muscle-invasive Bladder Cancer. Eur Urol. 2020;77(4):420-33.
19. Lindskrog SV, Prip F, Lamy P, Taber A, Groeneveld CS, Birkenkamp-Demtroder K, et al. An integrated multi-omics analysis identifies prognostic molecular subtypes of non-muscle-invasive bladder cancer. Nat Commun. 2021;12(1):2301.
20. Hurst CD, Alder O, Platt FM, Droop A, Stead LF, Burns JE, et al. Genomic Subtypes of Non-invasive Bladder Cancer with Distinct Metabolic Profile and Female Gender Bias in KDM6A Mutation Frequency. Cancer Cell. 2017;32(5):701-15 e7.
21. Robertson AG, Kim J, Al-Ahmadie H, Bellmunt J, Guo G, Cherniack AD, et al. Comprehensive Molecular Characterization of Muscle-Invasive Bladder Cancer. Cell. 2017;171(3):540-56 e25.
22. Porten SP. Epigenetic Alterations in Bladder Cancer. Curr Urol Rep. 2018;19(12):102.
23. Martinez VG, Munera-Maravilla E, Bernardini A, Rubio C, Suarez-Cabrera C, Segovia C, et al. Epigenetics of Bladder Cancer: Where Biomarkers and Therapeutic Targets Meet. Front Genet. 2019;10:1125.
24. Osterman CK, Milowsky MI. New and Emerging Therapies in the Management of Bladder Cancer. F1000Res. 2020;9.
25. Zhu Z, Cao F, Li X. Epigenetic Programming and Fetal Metabolic Programming. Front Endocrinol (Lausanne). 2019;10:764.

26. Loras A, Segovia C, Ruiz-Cerda JL. Epigenomic and Metabolomic Integration Reveals Dynamic Metabolic Regulation in Bladder Cancer. Cancers (Basel). 2021;13(11).
27. Loı¨c Vale´ry HF, Jean-Claude Lefeuvre,, Simberloff D. In search of a real definition of the biological invasion phenomenon itself. Biol Invasions. 2008;10:1345-51.
28. Narter KF, Sabuncu K. Invasion Mechanisms of Bladder Cancer: A moleculer Review Journal of Urological Surgery. 2016;3:66-73.
29. Zhu J, Tian Z, Li Y, Hua X, Zhang D, Li J, et al. ATG7 Promotes Bladder Cancer Invasion via Autophagy-Mediated Increased ARHGDIB mRNA Stability. Adv Sci (Weinh). 2019;6(8):1801927.
30. Wang P, Nishitani MA, Tanimoto S, Kishimoto T, Fukumori T, Takahashi M, et al. Bladder cancer cell invasion is enhanced by cross-talk with fibroblasts through hepatocyte growth factor. Urology. 2007;69(4):780-4.
31. Li Y. GG, Song J., Cai Z. et. al. B7-H3 Promotes the Migration and Invasion of Human Bladder Cancer Cells via the PI3K/Akt/STAT3 Signaling Pathway. Journal Of Cancer. 2017;8(5):816-25.
32. Chen W, Zhao K, Miao C, Xu A, Zhang J, Zhu J, et al. Silencing Trim59 inhibits invasion/migration and epithelial-to-mesenchymal transition via TGF-beta/Smad2/3 signaling pathway in bladder cancer cells. Onco Targets Ther. 2017;10:1503-12.
33. Li Y. ZW, Zhu M., Hu S. et. al. Nodal regulates bladder cancer cell migration and invasion via the AL K/Smad signaling pathway. OncoTargets and Therapy. 2018;11:6589–97.
34. Bolenz C, Knauf D, John A, Erben P, Steidler A, Schneider SW, et al. Decreased Invasion of Urothelial Carcinoma of the Bladder by Inhibition of Matrix-Metalloproteinase 7. Bladder Cancer. 2018;4(1):67-75.
35. Sayan AE, Stanford R, Vickery R, Grigorenko E, Diesch J, Kulbicki K, et al. Fra-1 controls motility of bladder cancer cells via transcriptional upregulation of the receptor tyrosine kinase AXL. Oncogene. 2012;31(12):1493-503.
36. Sylvester RJ. Bacillus Calmette-Guerin treatment of non-muscle invasive bladder cancer. Int J Urol. 2011;18(2):113-20.

37. Shore ND, Palou Redorta J, Robert G, Hutson TE, Cesari R, Hariharan S, et al. Non-muscle-invasive bladder cancer: An overview of potential new treatment options. Urol Oncol. 2021.
38. International Collaboration of T, Medical Research Council Advanced Bladder Cancer Working P, European Organisation for R, Treatment of Cancer Genito-Urinary Tract Cancer G, Australian Bladder Cancer Study G, National Cancer Institute of Canada Clinical Trials G, et al. International phase III trial assessing neoadjuvant cisplatin, methotrexate, and vinblastine chemotherapy for muscle-invasive bladder cancer: long-term results of the BA06 30894 trial. J Clin Oncol. 2011;29(16):2171-7.
39. Sonpavde G, Goldman BH, Speights VO, Lerner SP, Wood DP, Vogelzang NJ, et al. Quality of pathologic response and surgery correlate with survival for patients with completely resected bladder cancer after neoadjuvant chemotherapy. Cancer. 2009;115(18):4104-9.
40. Patel V. OW, Galsky M.D. Treatment of Muscle-Invasive and Advanced Bladder Cancer in 2020. CA Cancer J Clin. 2020(70):404-23.
41. Weber M, Hellmann I, Stadler MB, Ramos L, Paabo S, Rebhan M, et al. Distribution, silencing potential and evolutionary impact of promoter DNA methylation in the human genome. Nat Genet. 2007;39(4):457-66.
42. Lin X, Tirichine L, Bowler C. Protocol: Chromatin immunoprecipitation (ChIP) methodology to investigate histone modifications in two model diatom species. Plant Methods. 2012;8(1):48.
43. Rafiee MR, Sigismondo G, Kalxdorf M, Forster L, Brugger B, Bethune J, et al. Protease-resistant streptavidin for interaction proteomics. Mol Syst Biol. 2020;16(5):e9370.
44. Vial E, Sahai E, Marshall CJ. ERK-MAPK signaling coordinately regulates activity of Rac1 and RhoA for tumor cell motility. Cancer Cell. 2003;4(1):67-79.
45. Tsai HP, Tsai TH, Hsieh YJ, Chen YT, Lee CL, Tsai YC, et al. Overexpression of Fli-1 in astrocytoma is associated with poor prognosis. Oncotarget. 2017;8(17):29174-86.
46. Unpaired parametric t test GraphPad 8.3.0. ed. San Diego, California USA: GraphPad Software.

47. Li H, Durbin R. Fast and accurate short read alignment with Burrows-Wheeler transform. Bioinformatics. 2009;25(14):1754-60.

48. Heinz S, Benner C, Spann N, Bertolino E, Lin YC, Laslo P, et al. Simple combinations of lineage-determining transcription factors prime cis-regulatory elements required for macrophage and B cell identities. Mol Cell. 2010;38(4):576-89.

49. Zhang Y, Liu T, Meyer CA, Eeckhoute J, Johnson DS, Bernstein BE, et al. Model-based analysis of ChIP-Seq (MACS). Genome Biol. 2008;9(9):R137.

50. Frankish A, Diekhans M, Ferreira AM, Johnson R, Jungreis I, Loveland J, et al. GENCODE reference annotation for the human and mouse genomes. Nucleic Acids Res. 2019;47(D1):D766-D73.

51. Hepburn AC, Veeratterapillay R, Williamson SC, El-Sherif A, Sahay N, Thomas HD, et al. Side population in human non-muscle invasive bladder cancer enriches for cancer stem cells that are maintained by MAPK signalling. PLoS One. 2012;7(11):e50690.

52. Park HS, Lee S, Lee J, Shin HB, Yoo SM, Lee MS, et al. Suppression of CD81 promotes bladder cancer cell invasion through increased matrix metalloproteinase expression via extracellular signal-regulated kinase phosphorylation. Investig Clin Urol. 2019;60(5):396-404.

53. Jian W, Yamashita H, Cardenas D, Sonpavde G, Lerner S. Comparison of the 5637 human urothelial cancer cell line with a second-generation 5637 cell line for cancer therapy. Cancer Research. 2008;68(9 Supplement):2711-.

54. Ramakrishnan S, Huss W, Foster B, Ohm J, Wang J, Azabdaftari G, et al. Transcriptional changes associated with in vivo growth of muscle-invasive bladder cancer cell lines in nude mice. Am J Clin Exp Urol. 2018;6(3):138-48.

55. Stark R, Brown G.D,. DiffBind: differential binding analysis of ChIP-seq peak data. Bioconductor [Available from: http://bioconductor.org/packages/release/bioc/html/DiffBind.html.

56. Lawrence M, Huber W, Pages H, Aboyoun P, Carlson M, Gentleman R, et al. Software for computing and annotating genomic ranges. PLoS Comput Biol. 2013;9(8):e1003118.

57. Yu G, Wang LG, Han Y, He QY. clusterProfiler: an R package for comparing biological themes among gene clusters. OMICS. 2012;16(5):284-7.

58. Fishilevich S, Nudel R, Rappaport N, Hadar R, Plaschkes I, Iny Stein T, et al. GeneHancer: genome-wide integration of enhancers and target genes in GeneCards. Database (Oxford). 2017;2017.

59. UCSC Table Browser Tool [Available from: http://genome.ucsc.edu/cgi-bin/hgTables?hgta_doMainPage=1&hgta_group=regulation&hgta_track=geneHancer&hgta_table=geneHancer&hgsid=1136983873_cT0nak6vdCk33u54bpduD8J1jNAY.

60. Barretina J, Caponigro G, Stransky N, Venkatesan K, Margolin AA, Kim S, et al. The Cancer Cell Line Encyclopedia enables predictive modelling of anticancer drug sensitivity. Nature. 2012;483(7391):603-7.

61. Scrucca L, Fop M, Murphy TB, Raftery AE. mclust 5: Clustering, Classification and Density Estimation Using Gaussian Finite Mixture Models. R J. 2016;8(1):289-317.

62. Sjodahl G, Lauss M, Lovgren K, Chebil G, Gudjonsson S, Veerla S, et al. A molecular taxonomy for urothelial carcinoma. Clin Cancer Res. 2012;18(12):3377-86.

63. Ritchie ME, Phipson B, Wu D, Hu Y, Law CW, Shi W, et al. limma powers differential expression analyses for RNA-sequencing and microarray studies. Nucleic Acids Res. 2015;43(7):e47.

64. Wickham H. ggplot2: Elegant Graphics for Data Analysis. New York: Springer-Verlag; 2016.

65. Ramirez F, Ryan DP, Gruning B, Bhardwaj V, Kilpert F, Richter AS, et al. deepTools2: a next generation web server for deep-sequencing data analysis. Nucleic Acids Res. 2016;44(W1):W160-5.

66. Hahne F, Ivanek R. Visualizing Genomic Data Using Gviz and Bioconductor. In: In Mathé E DS, editor. Statistical Genomics: Methods and Protocols. New York: Springer New York; 2016. p. 335–51.

67. Bastian M, Heymann S., Jacomy M. Gephi: An Open Source Software for Exploring and Manipulating Networks. Proceedings of the International AAAI Conference on Web and Social Media2009. p. 361-2.

68. Tyanova S, Temu T, Cox J. The MaxQuant computational platform for mass spectrometry-based shotgun proteomics. Nat Protoc. 2016;11(12):2301-19.

69. Cancer Dependency Map; DepMap Broad Institute.

70. Lambert SA, Jolma A, Campitelli LF, Das PK, Yin Y, Albu M, et al. The Human Transcription Factors. Cell. 2018;175(2):598-9.
71. Xu J, Lamouille S, Derynck R. TGF-beta-induced epithelial to mesenchymal transition. Cell Res. 2009;19(2):156-72.
72. Loh CY, Chai JY, Tang TF, Wong WF, Sethi G, Shanmugam MK, et al. The E-Cadherin and N-Cadherin Switch in Epithelial-to-Mesenchymal Transition: Signaling, Therapeutic Implications, and Challenges. Cells. 2019;8(10).
73. Tam SY, Wu VWC, Law HKW. Hypoxia-Induced Epithelial-Mesenchymal Transition in Cancers: HIF-1alpha and Beyond. Front Oncol. 2020;10:486.
74. Shen J, Lv X, Zhang L. GRHL2 Acts as an Anti-Oncogene in Bladder Cancer by Regulating ZEB1 in Epithelial-Mesenchymal Transition (EMT) Process. Onco Targets Ther. 2020;13:2511-22.
75. Xiang J, Fu X, Ran W, Wang Z. Grhl2 reduces invasion and migration through inhibition of TGFbeta-induced EMT in gastric cancer. Oncogenesis. 2017;6(1):e284.
76. Yang Z, Wu D, Chen Y, Min Z, Quan Y. GRHL2 inhibits colorectal cancer progression and metastasis via oppressing epithelial-mesenchymal transition. Cancer Biol Ther. 2019;20(9):1195-205.
77. Paltoglou S, Das R, Townley SL, Hickey TE, Tarulli GA, Coutinho I, et al. Novel Androgen Receptor Coregulator GRHL2 Exerts Both Oncogenic and Antimetastatic Functions in Prostate Cancer. Cancer Res. 2017;77(13):3417-30.
78. Chung VY, Tan TZ, Tan M, Wong MK, Kuay KT, Yang Z, et al. GRHL2-miR-200-ZEB1 maintains the epithelial status of ovarian cancer through transcriptional regulation and histone modification. Sci Rep. 2016;6:19943.
79. Fishwick C, Higgins J, Percival-Alwyn L, Hustler A, Pearson J, Bastkowski S, et al. Heterarchy of transcription factors driving basal and luminal cell phenotypes in human urothelium. Cell Death Differ. 2017;24(5):809-18.
80. Choi W, Shah JB, Tran M, Svatek R, Marquis L, Lee IL, et al. p63 expression defines a lethal subset of muscle-invasive bladder cancers. PLoS One. 2012;7(1):e30206.
81. Wu Z, Xie Y, Bucher NL, Farmer SR. Conditional ectopic expression of C/EBP beta in NIH-3T3 cells induces PPAR gamma and stimulates adipogenesis. Genes Dev. 1995;9(19):2350-63.

82. Coutos-Thévenot L, Beji S, Neyret-Kahn H, Pippo Q, Fontugne J, Osz J, et al. PPARγ is a tumor suppressor in basal bladder tumors offering new potential therapeutic opportunities. bioRxiv. 2019:868190.
83. Cheng S, Qian K, Wang Y, Wang G, Liu X, Xiao Y, et al. PPARgamma inhibition regulates the cell cycle, proliferation and motility of bladder cancer cells. J Cell Mol Med. 2019;23(5):3724-36.
84. Goldstein JT, Berger AC, Shih J, Duke FF, Furst L, Kwiatkowski DJ, et al. Genomic Activation of PPARG Reveals a Candidate Therapeutic Axis in Bladder Cancer. Cancer Res. 2017;77(24):6987-98.
85. Desmet CJ, Gallenne T, Prieur A, Reyal F, Visser NL, Wittner BS, et al. Identification of a pharmacologically tractable Fra-1/ADORA2B axis promoting breast cancer metastasis. Proc Natl Acad Sci U S A. 2013;110(13):5139-44.
86. Diesch J, Sanij E, Gilan O, Love C, Tran H, Fleming NI, et al. Widespread FRA1-dependent control of mesenchymal transdifferentiation programs in colorectal cancer cells. PLoS One. 2014;9(3):e88950.
87. Zhang X, Wu J, Luo S, Lechler T, Zhang JY. FRA1 promotes squamous cell carcinoma growth and metastasis through distinct AKT and c-Jun dependent mechanisms. Oncotarget. 2016;7(23):34371-83.
88. Bejjani F, Tolza C, Boulanger M, Downes D, Romero R, Maqbool MA, et al. Fra-1 regulates its target genes via binding to remote enhancers without exerting major control on chromatin architecture in triple negative breast cancers. Nucleic Acids Res. 2021;49(5):2488-508.
89. Ben-David Y, Giddens EB, Letwin K, Bernstein A. Erythroleukemia induction by Friend murine leukemia virus: insertional activation of a new member of the ets gene family, Fli-1, closely linked to c-ets-1. Genes Dev. 1991;5(6):908-18.
90. Wilson NK, Foster SD, Wang X, Knezevic K, Schutte J, Kaimakis P, et al. Combinatorial transcriptional control in blood stem/progenitor cells: genome-wide analysis of ten major transcriptional regulators. Cell Stem Cell. 2010;7(4):532-44.
91. Li Y, Luo H, Liu T, Zacksenhaus E, Ben-David Y. The ets transcription factor Fli-1 in development, cancer and disease. Oncogene. 2015;34(16):2022-31.
92. Le Bras A, Samson C, Trentini M, Caetano B, Lelievre E, Mattot V, et al. VE-statin/egfl7 expression in endothelial cells is regulated by a distal enhancer and a

proximal promoter under the direct control of Erg and GATA-2. PLoS One. 2010;5(8):e12156.

93. Pimanda JE, Chan WY, Donaldson IJ, Bowen M, Green AR, Gottgens B. Endoglin expression in the endothelium is regulated by Fli-1, Erg, and Elf-1 acting on the promoter and a -8-kb enhancer. Blood. 2006;107(12):4737-45.

94. Tripolitsioti D, Kumar KS, Neve A, Migliavacca J, Capdeville C, Rushing EJ, et al. MAP4K4 controlled integrin beta1 activation and c-Met endocytosis are associated with invasive behavior of medulloblastoma cells. Oncotarget. 2018;9(33):23220-36.

95. Feng XJ, Pan Q, Wang SM, Pan YC, Wang Q, Zhang HH, et al. MAP4K4 promotes epithelial-mesenchymal transition and metastasis in hepatocellular carcinoma. Tumour Biol. 2016;37(8):11457-67.

96. Prolo LM, Li A, Owen SF, Parker JJ, Foshay K, Nitta RT, et al. Targeted genomic CRISPR-Cas9 screen identifies MAP4K4 as essential for glioblastoma invasion. Sci Rep. 2019;9(1):14020.

97. Ma B, Li H., Zhang C., Cai Q., Li G., Xu Y. Expression of MAP4K4 in bladder cancer and its biological effect on human bladder cancer T24 cells. Chinese Journal of Urology. 2014(12):469-72.

98. Guan Y, Song H, Zhang G, Ai X. Overexpression of flotillin-1 is involved in proliferation and recurrence of bladder transitional cell carcinoma. Oncol Rep. 2014;32(2):748-54.

99. Zhang L, Mao Y, Mao Q, Fan W, Xu L, Chen Y, et al. FLOT1 promotes tumor development, induces epithelial-mesenchymal transition, and modulates the cell cycle by regulating the Erk/Akt signaling pathway in lung adenocarcinoma. Thorac Cancer. 2019;10(4):909-17.

100. Jang D, Kwon H, Choi M, Lee J, Pak Y. Sumoylation of Flotillin-1 promotes EMT in metastatic prostate cancer by suppressing Snail degradation. Oncogene. 2019;38(17):3248-60.

101. Sokpor G, Xie Y, Rosenbusch J, Tuoc T. Chromatin Remodeling BAF (SWI/SNF) Complexes in Neural Development and Disorders. Front Mol Neurosci. 2017;10:243.

102. Nguyen H, Sokpor G, Pham L, Rosenbusch J, Stoykova A, Staiger JF, et al. Epigenetic regulation by BAF (mSWI/SNF) chromatin remodeling complexes is indispensable for embryonic development. Cell Cycle. 2016;15(10):1317-24.
103. Smith JM, Hedman AC, Sacks DB. IQGAPs choreograph cellular signaling from the membrane to the nucleus. Trends Cell Biol. 2015;25(3):171-84.
104. Nakazawa N, Sathe AR, Shivashankar GV, Sheetz MP. Matrix mechanics controls FHL2 movement to the nucleus to activate p21 expression. Proc Natl Acad Sci U S A. 2016;113(44):E6813-E22.
105. Chen Q, Kassab MA, Dantzer F, Yu X. PARP2 mediates branched poly ADP-ribosylation in response to DNA damage. Nat Commun. 2018;9(1):3233.
106. Gil-Kulik P, Dudzinska E, Radzikowska-Buchner E, Wawer J, Jojczuk M, Nogalski A, et al. Different regulation of PARP1, PARP2, PARP3 and TRPM2 genes expression in acute myeloid leukemia cells. BMC Cancer. 2020;20(1):435.
107. Gurski LA, Knowles LM, Basse PH, Maranchie JK, Watkins SC, Pilch J. Relocation of CLIC1 promotes tumor cell invasion and colonization of fibrin. Mol Cancer Res. 2015;13(2):273-80.
108. Li BP, Mao YT, Wang Z, Chen YY, Wang Y, Zhai CY, et al. CLIC1 Promotes the Progression of Gastric Cancer by Regulating the MAPK/AKT Pathways. Cell Physiol Biochem. 2018;46(3):907-24.
109. Fang ZQ, Zang WD, Chen R, Ye BW, Wang XW, Yi SH, et al. Gene expression profile and enrichment pathways in different stages of bladder cancer. Genet Mol Res. 2013;12(2):1479-89.
110. Kim Y, Hur SW, Jeong BC, Oh SH, Hwang YC, Kim SH, et al. The Fam50a positively regulates ameloblast differentiation via interacting with Runx2. J Cell Physiol. 2018;233(2):1512-22.

8. APPENDIX

PERİHAN YAĞMUR GÜNERİ SÖZERİ

Personal Information

Contact Information

Contact Address

Telephone

Email

Web Page

Education Information

31 July 2018 - Now (3 Year 1 Month)
Yüksek Lisans, Tezli Program, DOKUZ EYLÜL ÜNİVERSİTESİ, TÜRKİYE
İZMİR ULUSLARARASI BİYOTIP VE GENOM ENSTİTÜSÜ, MOLEKÜLER BİYOLOJİ VE GENETİK (YL) (TEZLİ) (İNGİLİZCE)
Diploma Number: -

04 September 2012 - 31 January 2018 (5 Year 5 Month)
Lisans, Anadal/Normal Öğretim, İSTANBUL TEKNİK ÜNİVERSİTESİ, TÜRKİYE
MOLEKÜLER BİYOLOJİ VE GENETİK BÖLÜMÜ, MOLEKÜLER BİYOLOJİ VE GENETİK PR. (İNGİLİZCE)
Diploma Number: 2018-01-0722
Cumulative Grade Point Average: 2.9 / 4.0

R&D Competency

Articles

A. ERAY, P. Y. GUENERİ, G. O. YİLMAZ, G. KARAKUELAH & S. ERKEK-OZHAN, Analysis of open chromatin regions in bladder cancer links beta-catenin mutations and Wnt signaling with neuronal subtype of bladder cancer, SCIENTIFIC REPORTS, 2020, 2045-2322, 10, 1.

Conference Papers

A. ERAY, P. Y. GÜNERİ SÖZERİ, G. ÖZDEN YILMAZ, G. KARAKÜLAH & S. ERKEK ÖZHAN, Analysis of ATAC-Seq data for bladder cancer reveals the link between WNT Pathway B-catenin mutations and neuronal subtype of bladder cancer, Poster Sunumu, EMBL Chromatin and Epigenetics, 17 May 2021, 20 May 2021.

A. ERAY, G. ÖZDEN YILMAZ, P. Y. GÜNERİ SÖZERİ & S. ERKEK ÖZHAN, İdrardan elde edilen üretalyal kök hücreler ile mesane kanserinin epigenetik regülasyonunun belirlenmesi, Sözlü Sunum, Okolojize İz Bırakanlar Zirvesi, 14 November 2019, 17 November 2019, 37 - 37.

P. Y. GÜNERİ SÖZERİ, G. ÖZDEN YILMAZ, A. ERAY, S. N. ATABEY, Ş. ŞENTÜRK & S. ERKEK ÖZHAN, İnvaziv olan ve invaziv olmayan mesane kanseri hücre hatlarını karakterize eden transkripsiyonel düzenleyici ağların tanımlanması, Sözlü Sunum, ONKOLOJİDE İZ BIRAKANLAR ZİRVESİ 2019, 14 November 2019, 17 November 2019, 38 - 38.

P. Y. GÜNERİ SÖZERİ, G. ÖZDEN YILMAZ, A. ERAY, S. N. ATABEY, Ş. ŞENTÜRK & S. ERKEK ÖZHAN, Identification of transcriptional regulatory networks characterizing invasive and non-invasive bladder cancer cell lines, Poster Sunumu, The International Symposium on Health Informatics and Bioinformatics, (HIBIT) 2019, 17 October 2019, 18 October 2019.

P. Y. GÜNERİ SÖZERİ, G. ÖZDEN YILMAZ, A. ERAY, S. N. ATABEY, Ş. ŞENTÜRK & S. ERKEK ÖZHAN, Identification of transcriptional regulatory networks characterizing invasive and non-invasive bladder cancer cell lines, Sözlü Sunum, International Bladder Cancer Network Annual Meeting 2019, 03 October 2019, 05 October 2019.

P. Y. GÜNERİ SÖZERİ, G. ÖZDEN YILMAZ, A. ERAY, S. N. ATABEY, Ş. ŞENTÜRK & S. ERKEK ÖZHAN, Identification of transcriptional regulatory networks characterizing invasive and non-invasive bladder cancer cell lines, Poster Sunumu, EMBO Young Scientists Forum 2019, 27 June 2019, 28 June 2019.

A. ERAY, G. ÖZDEN YILMAZ, P. Y. GÜNERİ SÖZERİ & S. ERKEK ÖZHAN, Pan-cancer analysis of UTX and MLL3 mutations in gene regulation, Poster Sunumu, 11th EMBO Young Scientists Forum, 27 June 2019, 28 June 2019.

TÜBİTAK Scholarships and Fundings

Project Info

118Z166, İnvazif Olan Ve İnvazif Olmayan Mesane Kanser Hücre Hatlarını Karakterize Eden Transkripsiyon Regülasyon Ağlarının Belirlenmesi, 3501 - Kariyer, Burslu, Yürürlükte, ARDEB, KBAG - Kimya Biyoloji Araştırma Destek Grubu, Project Participation/Leave Dates: 6/15/21 - 12/1/21, Project Start/End Dates: 12/1/18 - 12/1/21.
118Z166, İnvazif Olan Ve İnvazif Olmayan Mesane Kanser Hücre Hatlarını Karakterize Eden Transkripsiyon Regülasyon Ağlarının Belirlenmesi, 3501 - Kariyer, Burslu, Yürürlükte, ARDEB, KBAG - Kimya Biyoloji Araştırma Destek Grubu, Project Participation/Leave Dates: 12/1/20 - 5/1/21, Project Start/End Dates: 12/1/18 - 12/1/21.
118Z166, İnvazif Olan Ve İnvazif Olmayan Mesane Kanser Hücre Hatlarını Karakterize Eden Transkripsiyon Regülasyon Ağlarının Belirlenmesi, 3501 - Kariyer, Burslu, Yürürlükte, ARDEB, KBAG - Kimya Biyoloji Araştırma Destek Grubu, Project Participation/Leave Dates: 12/14/18 - 7/2/20, Project Start/End Dates: 12/1/18 - 12/1/21.

BIDEB Supports

PERİHAN YAĞMUR GÜNERİ SÖZERİ, Etkinlik Destekleri ve Eğitim Bursları Müdürlüğü, 2210-A Genel Yurt İçi Yüksek Lisans Burs Programı, Başvurusu Reddedildi, 2018 - 2, 10/1/18 - 9/30/20.

Number of Panelist/Observer/Reporter Jobs

Refereeing/Panelist/Outer Consultant Count	ARDEB/BİDEB 0	TEYDEB 0	Total 0
Number of Observer/Consultant Jobs	ARDEB/BİDEB 0	TEYDEB 0	Total 0
Number of Reporter Jobs	ARDEB/BİDEB 0	TEYDEB 0	Total 0